



Nutrient Emissions and Loads in the Danube River Basin

Current situation and scenarios for the 3rd Danube River Basin Management Plan – Final report

EU LIFE Project “Support for the Development of the 3rd Danube River Basin Management and 2nd Flood risk Management Plan Update 2021” (*LIFE19 PRE AT 006 – LIFE DRBMP DFRMP 2021*)

Client:

Permanent Secretariat of the International Commission for the Protection of the Danube River (ICPDR), Vienna

Contractor:

Leibniz-Institute for Freshwater Ecology and Inland Fisheries (IGB)

Andreas Gericke and Markus Venohr

Müggelseedamm 310

12587 Berlin, Germany

2 December 2021

Content

List of abbreviations	3
Summary	4
1 Rationale.....	5
2 Model revision and model setup.....	5
2.1 Overview of model modifications since the application for the 2 nd DRBMP	6
2.2 Analytical units – Delineation and flow direction (routing)	7
2.3 Input data	8
2.3.1 Hydrology	8
2.3.2 River network	11
2.3.3 Agricultural nitrogen balance	12
2.3.4 Point source: Waste-water treatment plants (WWTP) and industrial dischargers.....	15
2.3.5 Total population and connection rates to waste-water collection and treatment	16
2.3.6 Soil erosion	19
2.3.7 Further data updates compared to previous database	20
2.4 Observation data	24
2.5 Scenario implementation	24
2.5.1 Baseline scenario	24
2.5.2 Vision I scenario.....	27
2.5.3 Vision II and III scenarios	28
3 Model results.....	28
3.1 Spatial variability of nutrient emission.....	29
3.2 Contribution of emission pathways	31
3.3 Nutrient load and load comparison	39
3.4 Scenario results	42
3.5 Conclusions and recommendations	44
3.6 Acknowledgements	45
4 References.....	46
5 Appendix.....	48

List of abbreviations

Throughout the report, we use the two-letter country codes according to ISO 3166-1 alpha-2 and the abbreviated names of models and datasets.

Names of emission pathways in MONERIS

AD	atmospheric deposition (on surface water)
ER	soil erosion
TD	tile drainage
SR	surface runoff
GW	groundwater (subsurface flow)
US	urban systems
PS	point sources (waste-water treatment plants and industrial dischargers)

Other abbreviations

AU	analytical (modelling) unit (of MONERIS)
DCTP	decentralized (independent) treatment plant
DP	discharge point (e.g. of sewer systems)
DRB	Danube River Basin
DRBMP	DRB Management Plan
E-PRTR	European Pollutant Release and Transfer Register
kt	kilo tons
MR	main rivers (which connect AUs)
N	nitrogen
NVZ	Nitrate Vulnerable Zone
P	phosphorus
p. e.	population equivalent
TN	total nitrogen
TNMN	Trans-National Monitoring Network
TP	total phosphorus
UWWTD	Urban Waste-Water Treatment Directive (of the European Union)
USLE	universal soil loss equation
WSP	water soluble phosphorus
WWTP	waste-water treatment plant

Summary

We estimated the amount of nutrients entering the surface waters (emissions) as well as in the surface waters (load). We specifically addressed emissions and loads of nitrogen and phosphorus in the whole Danube River Basin. For this purpose, we used the established model MONERIS and comprehensively updated the previous model setup in close collaboration with ICPDR as well as national and other experts. In a first step, we adjusted the modelling units to the outlines of the Danube Basin and its sub-catchments and collected data for the new reference period 2015-2018. After comparing the modelled loads to observed loads, we modified the MONERIS database for one Baseline and four mid- to long-term Vision scenario calculations. While the Baseline scenario considered possible changes until 2027 based on country and ICPDR, the Vision scenarios were what-if assessments of ambitious actions to lower agricultural and urban emissions.

Under current conditions, about 513.000 tons nitrogen and 31.000 tons phosphorus enter each year the surface waters within the Danube River Basin. Agricultural land and urban areas contribute more than 30% which makes them the dominant sources. Groundwater and soil erosion are the main pathways for nitrogen and phosphorus, respectively, followed by urban systems and point sources. This is in agreement with previous MONERIS applications. However, the considerable change and revision of input data hampers the comparison. The loads and concentrations exported to the Black Sea are currently close to the target values. They can considerably be (further) reduced by lowering the agricultural N surplus, by soil conservation, and more effective waste-water collection and treatment. However, these measures may become less effective if intense rainfall and high-flood events become more frequent.

It is important to keep in mind that any model is a simplification of the complex reality, especially if it has to be applied to such a large and diverse river basin as the Danube River Basin. Our estimations were based on numerous international and national datasets, and where both were missing, assumptions. The available data differed in resolution, type, and underlying assumptions. Therefore, one of our primary goals was the acceptance of the model results. We addressed this by integrating national data and communicating the model needs, assumptions and outcomes, as well as data issues. Accordingly, this report provides technical information on the model setup, basin-wide and country-specific model results, and recommendations for future collaborations.

1 Rationale

The modelling aimed at estimating the nutrient emissions to surface waters within the Danube River Basin (DRB) via different pathways and the resultant loads. The results served as input for the 3rd DRB Management Plan (DRBMP). For this purpose, we comprehensively updated the setup of the model MONERIS (Venohr et al., 2011) for the previous DRBMP. To foster the acceptance of the results, the input data was collected in close collaboration with ICPDR and the national experts of the ICPDR groups PM EG and NTG. During the data collection, suspicious data were communicated to ICPDR and external authorities and various issues could be fixed. The estimated nitrogen (N) loads for the reference period (2015–18) were successfully validated with loads derived from observation data. For phosphorus (P), we used the observed data to re-calibrate the in-stream retention as the previous and current MONERIS approaches either under- or overestimated the observed loads. Based on the setup for the reference period, we implemented four scenarios to assess basin-wide effects of measurements as well as hydrological changes.

Due to the many changes in the model database, we do not recommend comparisons to previous model results. The changes in the emissions and the relevance of pathways will reflect partly real changes but also changes in the input data and the assumptions underlying this data. The decision to use certain national datasets (if available) was a trade-off between the resources needed for a broader data collection and the preprocessing, the national acceptance, as well as the consistency among countries. The availability and resolution of input data differed among the countries as well as the area of the modelling units which hamper the comparison of countries. Likewise, the basin-wide application should not be compared to national assessments based on more detailed input data.

2 Model revision and model setup

This chapter provides an overview of the recent developments of the MONERIS model and the revised input database for the reference period 2015–2018 followed by the implementation of four scenarios. The model needs data for each analytical unit (AU), i.e. its basic modelling units. If (new) data was unavailable, we either relied on the existing model database (e.g. tile drainage) or filled gaps with (updated) data from neighboring countries (e.g. N balance in BA).

The existing database for the previous reference period 2009–2012 had to be adjusted to new AU geometries which were derived from revised sub-catchment boundaries. With the data update, we also fixed two mistakes in the previous database. Although the inventory of waste-water treatment plants (WWTP) was again taken from the UWWTD database collected by ICPDR, the current database was firstly derived from discharge points of WWTPs (connection type “ISCON”) instead of agglomerations (which include sewer systems without WWTPs, i.e. connection type “NOTCON”). This correction resulted in lower emissions via point sources. Secondly, the gross agricultural N balances were replaced by net balances which lowered the N emissions via groundwater and tile drainage. In addition, the N balances (in kg/ha utilized agricultural land) were corrected for the difference between the agricultural land used by MONERIS and the agricultural statistics. This further reduced the modelled N emissions because the first was typically larger than the latter.

After discussing the limitations of local water discharge being estimated from station data with ICPDR and national experts, we were able to make use of modelled water fluxes from catchments to local streams and modelled water discharges which resulted in more acceptable spatial pattern.

Unfortunately, the hydrological data was only available for the years 2003–2013. Therefore, MONERIS could only be run and validated with multi-annual mean values.¹

2.1 Overview of model modifications since the application for the 2nd DRBMP

Since the application for the previous DRBMP, MONERIS was modified regarding

- P emission via surface runoff

The new approach is based on water-soluble P (WSP), after Vadas et al. (2005) and Fischer et al. (2017). WSP is a new model input and replaces P accumulation. It is normally unavailable but can be estimated from plant-available P for which various national standards exist in the DRB. Various regression models had been proposed (e.g. Schick et al., 2013), which differ considerably. We agreed with the few providers of plant-available P (CZ, DE, SI, and SK) to refrain from using the national data in favor of a Europe-wide estimation (Lemm et al., 2021). The new approach resulted in higher TP emissions via surface runoff compared to the previous model application (Table 1).

Table 1. P emission via surface runoff from arable land, 2009–2012, in tons

	Previous model run	Previous database with WSP
Median	0.05	0.18
Mean	0.19	0.73
Maximum	6.27	34.5

- Emission via soil erosion

A fixed enrichment ratio of 1.86 is now used (Wilke and Schaub, 1996). The sediment delivery ratio is also applied to forested land.

- P instream retention / remobilization

While the previous DRB approach underestimated the P load, the more recent approach developed in the EU MARS project (Lemm et al., 2021) overestimated the P load. Therefore, the in-stream retention was re-calibrated using observation data from 18 stations in 17 AUs² (cf. sections 2.4 & 3.3). The net retention was conceptually split into gross retention (sedimentation) and remobilization. The sedimentation is derived from the hydraulic load (HL, in m/month) which is the ratio of water discharge (Q, m³/month) and water surface area (m²) (cf. Venohr et al., 2011). For main rivers (MR), we took the average slope (β , %) into consideration assuming that the retention is higher in flat terrain than in steep terrain.

$$R_{TP,MR} = 1 - (60/\beta \text{ HL}_{MR}^{-1})^{-1}$$

$$R_{TP,Trib} = 1 - (60 \text{ HL}_{Trib}^{-1})^{-1}$$

For the remobilization, we used the current sedimentation and separate sediment pools for MR and tributaries which were filled during a preliminary run as well as the ratio of average Q and current Q. The share of remobilized P was calculated for MRs and tributaries as

$$S_{TP} = 1/(1 + 585(\bar{Q}/Q_{mon})^2)$$

¹ MONERIS can either be applied for specific years or average (“long-term”) conditions.

² The TNMN stations DE2 and AT1 at Jochenstein (Danube) are located in the same AU.

- Buffer retention

The nutrient retention in riparian buffers was not only applied to emissions via soil erosion but also to emissions via surface runoff. Although riparian buffers also interact with nutrients in subsurface flow, the groundwater pathway of MONERIS could conceptually not (yet) be considered.

2.2 Analytical units – Delineation and flow direction (routing)

The existing MONERIS AUs were adjusted to the latest DRB boundary (its final version was provided end of August 2021 by ICPDR) and to national boundaries of sub-catchments. The original sub-catchments had flaws which required various processing steps:

- Fewer sub-catchments than the previous analytical units which resulted in
- Many large areas which were deemed to be unsuitable for load calculation and validation
- Overlaps and gaps between many countries often due to inaccurate (re-)projection
- Sub-catchments consisting of multiple parts
- Missing areas, e.g. in CZ and ME
- Unsuitable and missing values for the downstream neighbor

The new AUs were derived by overlaying the sub-catchments and the existing AUs. An iterative, semi-manual approach targeted tiny areas and other artefacts. The geometric issues could be reduced but not completely fixed. The AU boundaries were partly adjusted to monitoring stations and the river network. Finally, 1727 new AUs were created, i.e. 149 more than previously used. The new AUs conserved the area of the sub-catchments (Figure 1 left) despite the removed gaps and overlaps.

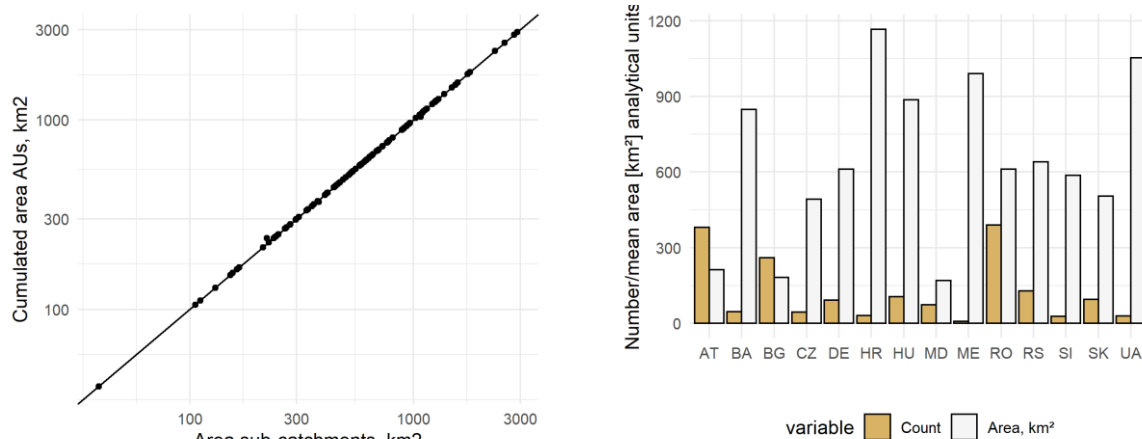


Figure 1. The revised AUs almost perfectly match the national sub-catchments (left), their number and area vary among the countries (right).

The number and areas of AUs differed widely among the Danube countries (Figure 1 right). Their areas ranged from 1.2 to 4600 km² (compared to 0.2–10500 km² for the previous AUs and 0.8–16000 km² for the sub-catchments). Although not a computational problem, large areas may hide the spatial variability of nutrient emissions.

The AUs need a flow direction for the load calculation. For this purpose, we compared the reported catchment areas of monitoring stations with the total upstream AU areas. The derived and manually revised AU network was a directed, acyclic graph without splittings like canals, i.e. AUs with more than one downstream neighbor. The final water flow of AUs was not necessarily in line with the sub-catchments. Flow deviations typically occurred along borders as sub-catchments rarely had valid foreign downstream neighbors, thus resulting in parallel flow e.g. along the Danube in Romania and

Bulgaria. In contrast, the AUs had to collect water across borders. In case of the lower Danube, Bulgarian AUs generally flow into the Romanian AUs.

More than 1000 stations were provided by the countries and assigned to AUs. To reduce the workload, small station catchments were excluded as the stations typically represent single AUs, if any. The ratios of cumulate AU areas and reported catchment areas were calculated. The catchments of stations not located near AU outlets were approximated by the sum or difference of multiple AUs. Large deviations from 1.0 (perfect agreement) occurred for three reasons: wrong water flow of AUs, wrong assignment (or inadequate geometry of AUs), wrong catchment areas of stations. All issues were addressed until the water flow was found to be plausible. However, local errors may still exist.

2.3 Input data

For the modelling, we considered input data provided until the beginning of September 2021. In November 2021, the loads of a few WWTPs in UA and SI were revised.

2.3.1 Hydrology

Water discharge is a key input for MONERIS. Without a proper hydrological model, previous model applications relied on simple water balancing using the available monitoring data. While the estimated fitted nicely the observed discharge, this approach could not reliably produce spatial patterns due to the complex hydrology and missing data for the balancing (e.g. water diversion and abstraction for irrigation). For the current modelling, we cooperated with J. van Gils (Deltares) who provided a subset of the compiled output of a Europe-wide application of the HYPE model (E-HYPE, Table 2) (van Gils et al., 2020) – a dynamic and semi-distributed hydrological model (Swedish Meteorological and Hydrological Institute, 2020). The E-HYPE output was available for 3477 sub-catchments of the DRB for the years 2003–13. The AU values were derived by overlaying the HYPE areas and area weighting. Some AUs, mostly in BA and HR, were only partially covered by the E-HYPE units (Figure 2). Here we assumed that the small overlaps were representative for the whole AUs.

Table 2. HYPE datasets used for MONERIS. The first dataset (cumulated flow downstream) was also used for validating HYPE. The other datasets describe the water flux to local streams (ToLayer=STR) and point sources to main rivers (RIV).

Name HYPE data	FromLayer	ToLayer	From Subid	To Subid
Flowtomaindownstreamsubbasin	OLK	RIV	local	Maindown
Rainthatbecomesurfacerrunoff	SRO	STR	local	local
Snowmeltwaterthatbecomesurfacerrunoff	SNO	STR	local	local
Glacierrunoffwaterthatbecomesurfacerrunoff	GLA	STR	local	local
Surfacerrunoff(saturatedoverlandflow)	S1	STR	local	local
Groundwaterrunoff	S1–3	STR	local	local
Tiledrainage	S1–3	STR	local	local
Pointsource	PS	RIV	local	local
Ruraldiffusesource	DS	STR	local	local

Given the Europe-wide application and the different modelling periods to MONERIS, we validated the HYPE discharge to average monthly observed values. As the data was only available in May 2021, we

used the readily available TNMN data for validation, and found acceptable results within a range of $\pm 30\%$ (Figure 2). The main exception was the regulated r. Sió, the outflow of Lake Balaton.

For MONERIS, we calculated the local water discharge (or runoff) from AUs (Figure 6) from the water fluxes to local streams and used its implemented approaches to estimate the water fluxes for the different nutrient pathways. The difference between the water discharge at the outlet of sub-catchments and the local water fluxes was considered as (positive or negative) water addition.

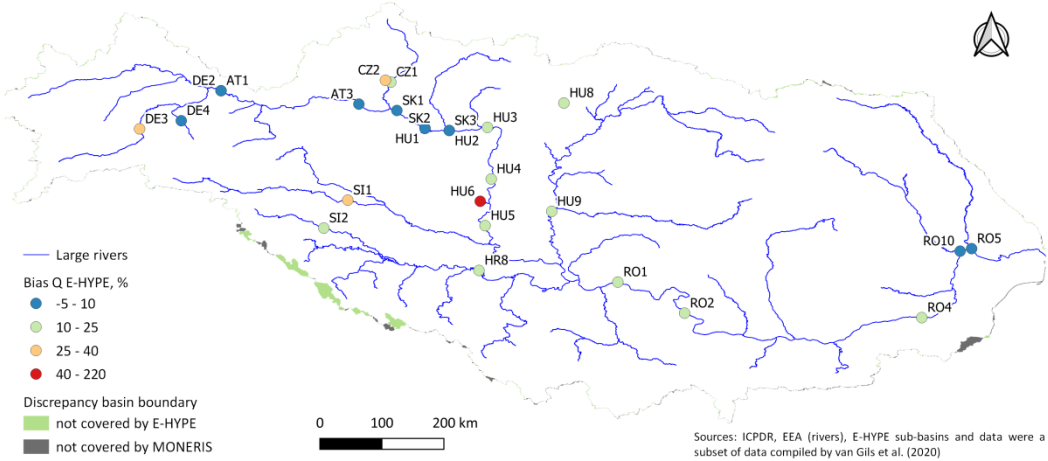


Figure 2. The extent of the DRB differed for E-HYPE and MONERIS. E-HYPE mostly overestimated the discharge at TNMN stations. The deviation (bias) for each station was derived from the monthly discharge 2003–2013.

HYPE overestimated the discharge in the reference period 2015–2018. To facilitate the load comparison and to avoid a general overestimation of emissions we derived monthly factors to adjust the modelled discharge (in m^3/s) from 114 stations (ids) in 91 AUs (Figure 3). The basin-wide adjustment resulted in a good agreement along the Danube but not necessarily along the tributaries (Figure 4).

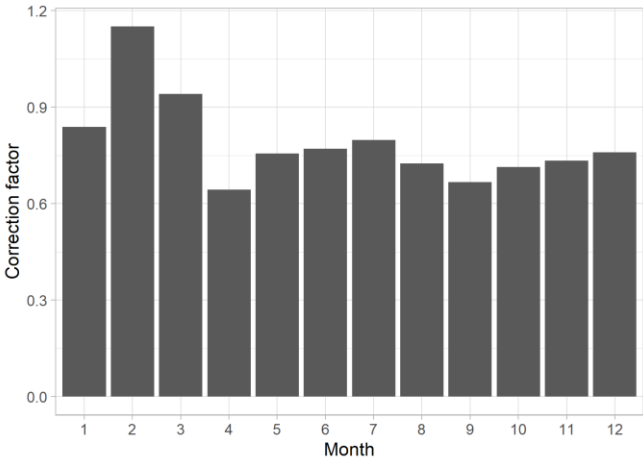


Figure 3. Correction factors to adjust the modelled discharge to the reference period.

The effect of changing the reference period as well as the modelling approach on hydrology differed considerably among the countries. Most noticeable were the higher discharge in ME and the lower discharge in MD and BG compared to the water-balancing approach (Figure 5). These impacts could be related to limitations of the water balancing, i.e. an underestimation of mountainous Montenegrin rivers due to the missing stations or negative flow balances due to reservoirs along r. Prut.

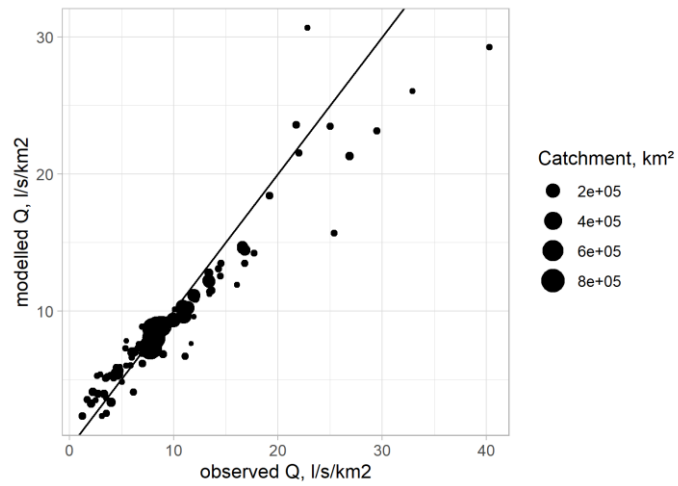


Figure 4. Comparison of area-specific water discharge after the model adjustment.

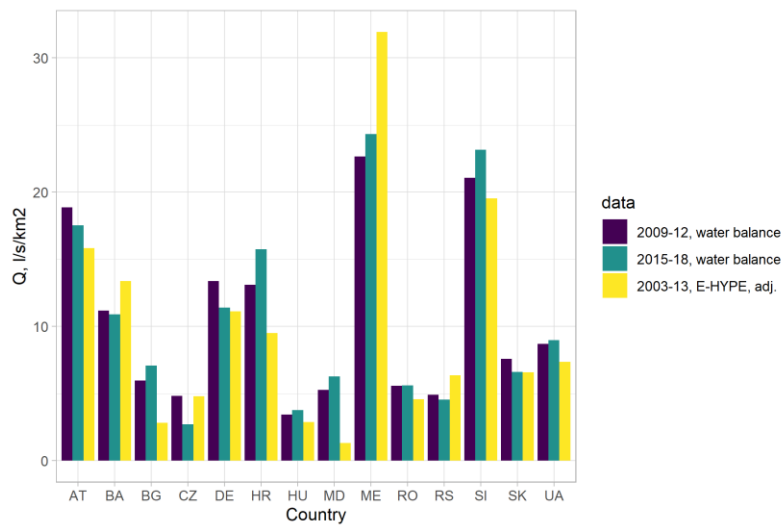


Figure 5. Basin-wide discharge for different time periods and modelling approaches. 2009-12 is last MONERIS application.

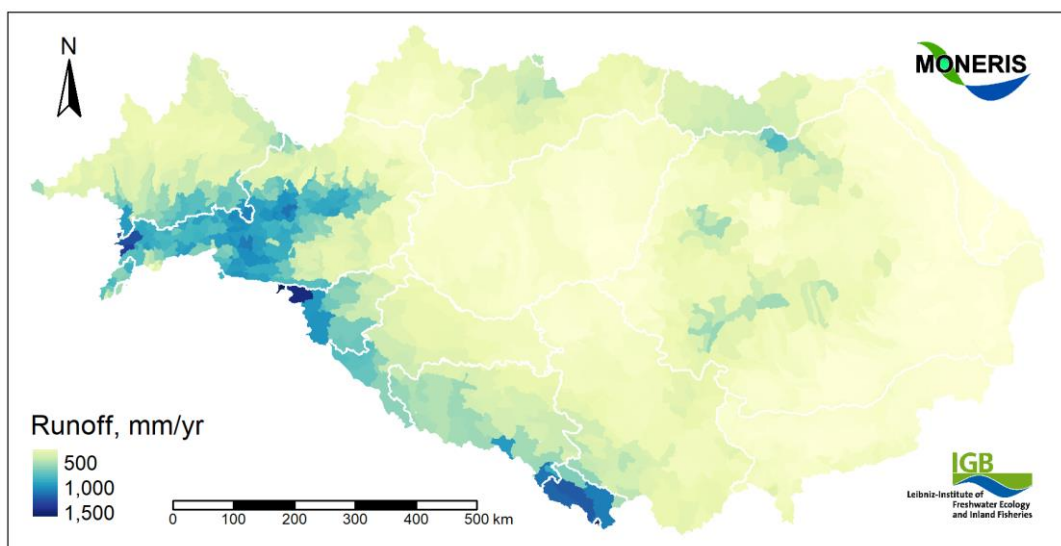


Figure 6. Annual water runoff from AUs used by MONERIS, HYPE data adjusted to 2015–2018.

2.3.2 River network

MONERIS distinguishes main rivers (MR) connecting AUs and tributaries. A few river networks were evaluated but all had their (dis-)advantages. We eventually used the ECRINS river network (European Environment Agency, 2012). Its rivers had been derived from a digital elevation model and can therefore deviate from their true locations. This was frequently observed in HU and RS. Additionally, ECRINS lacked canals and the extent of streams (polylines not polygons) but comprised lakes and reservoirs. MONERIS estimated the areas for the polylines.

The main rivers were semi-automatically delineated and assigned to the correct AUs. The assignment had to take into consideration the inaccuracy of the streams as well as the flow direction at AU level, especially along borders. Similarly, the polygons of lakes and reservoirs were assigned.

Table 3. Mean density of tributaries within the DRB as used to estimate the length of missing tributaries in AUs.

Country	Density km/km ²	Country	Density km/km ²	Country	Density km/km ²
AT	0.430	CZ	0.295	RO	0.283
BA	0.430	HU	0.191	RS	0.275
BG	0.290	MD	0.248	SI	0.443

We tested for plausibility to ensure that headwater AUs (upstream area = 0) had tributaries but no main rivers and that all other AUs had main rivers. For 21 AUs, we estimated missing tributaries (18 cases) and main rivers (4 cases). Apart from 9 small AUs (<20 km²) in AT, BG, CZ, HU, MD, and SI, tributaries were missing in large AUs in BA, HU, RS, and RO. Here we used the mean density of tributaries to estimate their lengths (Table 3). The lengths of missing main rivers (in RS) were obtained from OpenStreetMap (OSM) (geofabrik GmbH and OpenStreetMap Contributors, 2018).

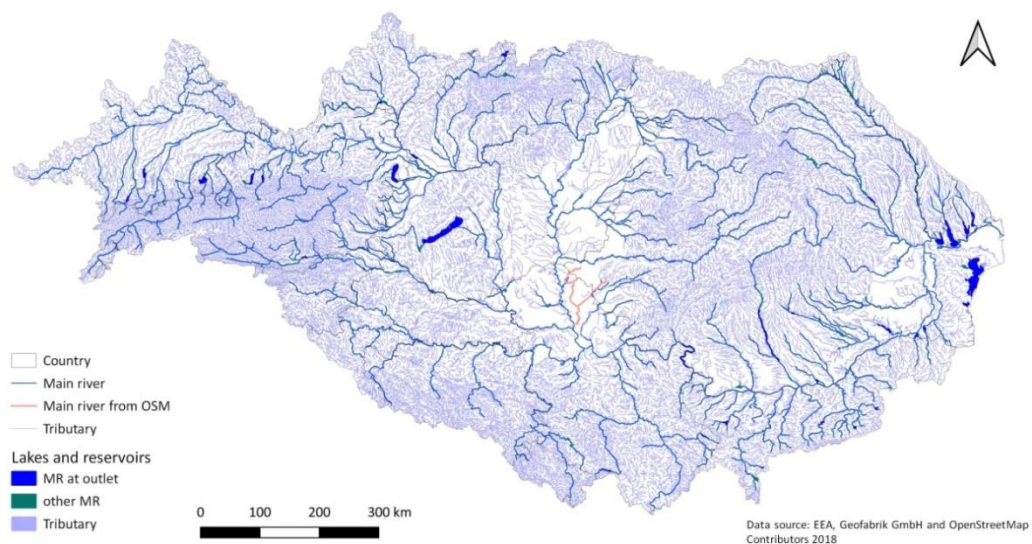


Figure 7. Main rivers and tributaries for MONERIS. Note the high stream density in AT and ME.

As expected, ECRINS underestimated the “true” length of rivers. The dataset was intended to correspond to a map scale of 1:250000 (European Environment Agency, 2012) which was confirmed by our comparison of the stream lengths to exemplary national (Federal Ministry of Agriculture, 2020, GeoBasis-DE and Federal Agency for Cartography and Geodesy, 2013) and OSM datasets. The average ratios of country or OSM lengths and ECRINS lengths were 1.05 for main rivers and 3.01 for tributaries (Figure 8). These values were close to the pre-defined MONERIS coefficients of 1.11 and 3.23 for this map scale.

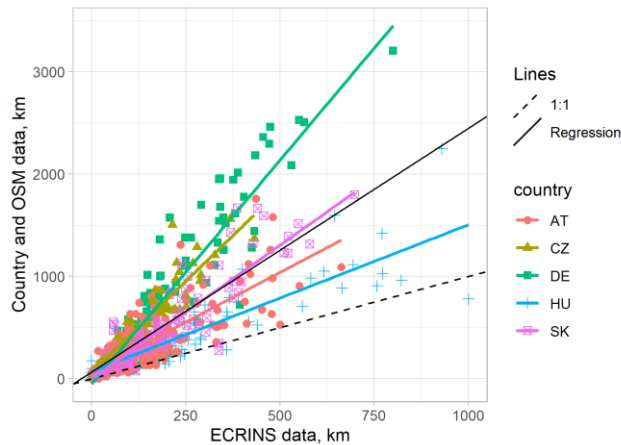


Figure 8. ECRINS underestimates the stream length within the DRB compared to detailed national (AT and DE) and OpenStreetMap data (OSM, for HU, SK, and CZ). Each point represents the lengths of main rivers and tributaries per AU. The different slopes reflect not only variable stream densities in ECRINS but also in the networks used for comparison.

2.3.3 Agricultural nitrogen balance

The previous model applications showed that groundwater is the main pathway for N emissions in the DRB. Excess nitrogen enters the groundwater (i.e. subsurface water) and tile drainages.³ However, due to the residence time of groundwater, the N emission for a given year only partially depend on the current N balances but rather on previous, often much higher N balances. MONERIS adjusts the regional values for a common reference year with multi-decadal time-series typically only available at national level. The relative change to the reference year in the time-series is used to adjust regional values:

$$N_{AU,year} = N_{AU,ref_year} \cdot N_{cnt,year} / N_{cnt,ref_year}$$

In contrast to the previous setup,

- regional balances were available for most countries which were adjusted by
- replacing the atmospheric deposition by the MONERIS input, i.e. from EMEP
- replacing the utilized agricultural area from the agricultural statistics by the agricultural land as used by MONERIS, i.e. arable and grass land as derived from the land-use/cover maps.

The provided regional N balances were net balances, i.e. gross balance without the gaseous losses. The differences between gross and net balances differed widely, from <2 kg/ha in parts of AT to >30 kg/ha in SI. They did hardly vary in CZ, but ranged from <2 to >20 kg/ha in AT. The exception was HU. Its balances were derived from agri-environmental diaries. They were considered as net balances without atmospheric deposition and without area adjustment as the fraction of the agricultural land they represent was unknown.

The MONERIS approach works well with positive N balances (N surplus) but is limited if either N_{cnt,ref_year} or N_{AU,ref_year} are negative (N deficit). Negative regional values appeared in various countries. This was mostly relevant for RO, but also in parts of HU, MD, and UA and presumably exhibited issues with the balances.⁴ Instead of setting negative regional balances to just above zero, we therefore spatially aggregated neighboring administrative units, except for HU where the (slightly) negative value was set to 0.1 kg/ha. The missing values for BA (and for ME) were estimated as average of HR and RS (A. Ibrulj,

³ In MONERIS without the atmospheric deposition which is a separate pathway.

⁴ For instance, the transport and application of manure were supposedly only estimated at the regional scale.

pers. comm., 31.3.21), i.e. 19.065 kg/ha (+ atmospheric deposition). For the few Czech AUs without data, we used the national average of 52.89 kg/ha (+ atmospheric deposition). Figure 9 shows the final model input for the reference year 2015. Missing values for this year were estimated from other years using the equation above.

The different data providers (Table 4) used different data and assumptions which influenced to an unknown degree the (national) N emissions. This was most obvious for the German federal states but was also indicated by the differences between the provided regional data and other national values.

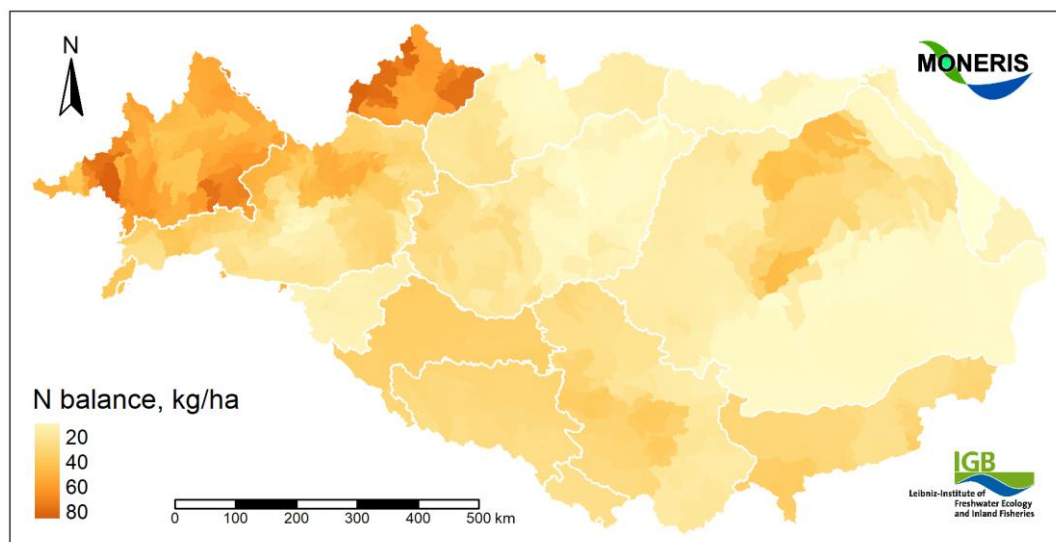


Figure 9. Agricultural N surplus for the reference year 2015, adjusted to the agricultural land in MONERIS and with filled gaps. Negative values were removed by spatially aggregating administrative units.

Table 4. Available regional N balances. Values reported for time periods indicated as ‘.’. The reference year for MONERIS was 2015. Missing values estimated with the relative annual change according to Table 5.

Country	2015	2016	2017	2018	Data provider	Estimation
AT	x	x	x	x	O. Zoboli, TU Vienna	
BA						Mean RS+HR
BG	x	x	x	x	O. Zoboli, TU Vienna	
CZ				x	National	
DE-BW	.	.			National, 2014–16, only net balances	
DE-BY			.	.	State agency, 2017–19, only net balances	
HR	x	x	x		Eurostat	cf. Table 5
HU		.	.	.	National, agro-enviro. Diaries, 2016–18	
MD			.	.	O. Zoboli, TU Vienna, data 2016–18	
RO	x	x	x	x	O. Zoboli, TU Vienna	
RS	x	x	x	x	O. Zoboli, TU Vienna	
SI	x	x	x	x	National	
SK	x	x	x	x	National	
UA				x	National	

National time-series since the 1990s were available for EU countries (Eurostat, 2021a) and for UA (OECD, 2021). The values replaced⁵ and extended the existing multi-decadal time series in MONERIS. We chose 2015 as reference year because a) no national balance had to be estimated, and b) all values were positive. The gaps in the Eurostat time-series were filled, e.g. with data from neighboring countries (assuming a similar trend) or the regional data (cf. Table 5). Regional balances which were not available for the reference year were estimated from the other years using the above equation and the time-series.

Table 5. National net N balances (in kg/ha) for 2015–2018 with missing values being estimated (red). Estimations are based on linear relationships to summer precipitation (May–Oct 2013–2017), regional data, or neighboring countries. The relative changes are used to adjust regional values which might differ.

Country	2015	2016	2017	2018	Comment (estimation)
AT	23.2	8.2	22.4	28	Regional data (O. Zoboli, TU Vienna)
BA					Similar to mean RS
BG	21.8	19.6	15.5	16.0	Very high value 2017 probably inconsistent, estimated as regional gross balance (O. Zoboli, TU Vienna) – 11.31 – 6.17 ^a
CZ	81.2	73.7	85.1	75	Regional value (O. Zoboli, TU Vienna)
DE ^b	89.9	85.2	77.2	102	Summer precipitation
HR	43.3	18.6	55.6	38 ^c	Summer precipitation
HU	21.9	14.2	18.6	22	Summer precipitation
MD					Similar to UA
RO	8.6	0.1	-10.3	4	Gross balance because all net balances negative, 2016 0 changed to 0.1
RS	27.8	13.9	44.1	24.6	Average of HR and SI
SI	12.3	9.3	32.6	11.3	
SK	24	2	19.1	8	Revised net balances Eurostat with very low values for 2014 and 2016 confirmed by national authority (P. S. Clausen, Eurostat, pers. comm., 23.6.21)
UA	6.7	6.9	13.1	12.2	OECD gross balance, gaseous losses unavailable, with RO values many negative estimates of net balances

^a national average (TU Vienna) – Eurostat 2015 = 11.31 kg/ha, average gaseous losses Eurostat 2012–2014 = 6.17 kg/ha ^b for DE-BY, strongly correlated to DE-BW and DE, ^c $r^2 \sim 0$, estimate is approx. mean value for 2013–2017.

Some time-series were seemingly inconsistent. For DE, the atmospheric deposition in 2017–2018 dropped by 7 kg/ha due to new input data. For the sake of consistency, also with the existing time-series, we used a different national modelling (Länderinitiative Kernindikatoren, 2020). For BG, the N input in 2017 (+50% compared to 2015) and the atmospheric deposition (+6 kg/ha) were likely inconsistent as well. Due to missing values for 2016 and 2018, we used the mean regional values instead of gap filling.

Due to the frequent negative net balances, we applied a time-series of gross balances for RO. For UA, only gross balances were available.

⁵ We switched from gross to net balances. However, gross balances also changed in the meantime, e.g. for RO.

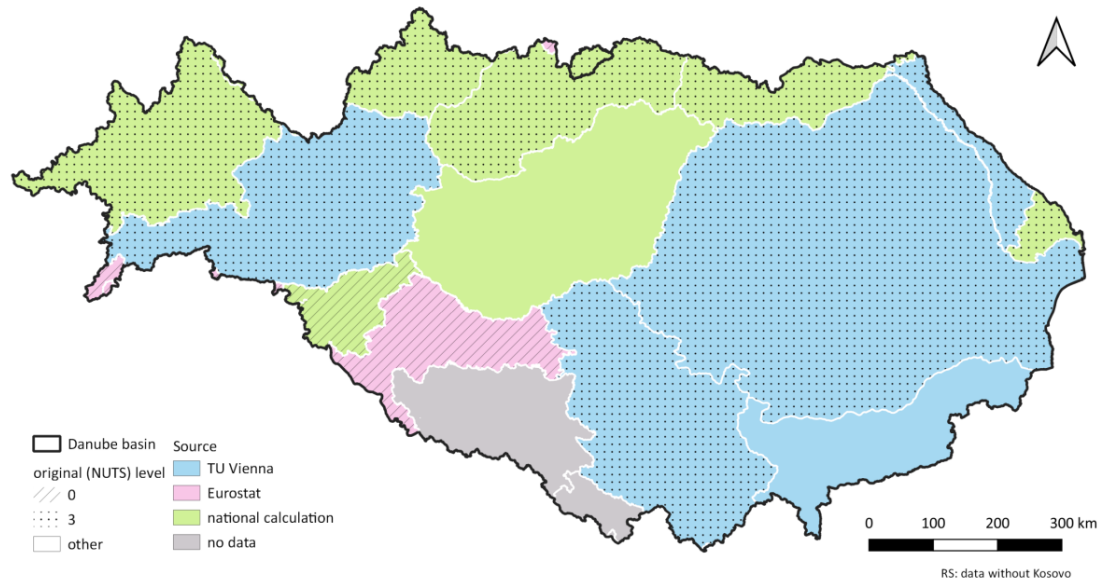


Figure 10. Overview of the data sources and original resolution of the regional N balances.

2.3.4 Point source: Waste-water treatment plants (WWTP) and industrial dischargers

From the latest UWWTD database, ICPDR created a table of discharge points (DP) of WWTPs (connection type = ISCON) with their coordinates as well as water volumes (in m³) and nutrient emissions (in tons). For most countries, the data was for the year 2018. We intersected the DPs and the AUs and corrected the assignments where the country of DPs and AUs differed. The loads were converted to concentrations. We assumed no annual changes at AU level.

The use of DPs instead of agglomerations was the main difference to the previous MONERIS setup. As agglomerations also include DPs of sewer systems without waste-water treatment (connection type = NOTCON), the new setup resulted in lower emissions via point sources. NOTCON comprised 7% of the basin-wide water volume, 25% of the N emissions, and 35% of P emissions, with large national differences. The WWTP inventory in MONERIS consisted of 3236 records including 28 records for IT, PL, and CH.

In absence of a basin-wide inventory of industrial dischargers, we used E-PRTR which covered the EU countries, RS, and CH. The database for the years 2007–2017 (European Environment Agency, 2020) was complemented with a database for 2017–2018 (European Environment Agency, 2021b) and by 7 records for BA (6) and UA (1) provided in September 2021 by ICPDR. E-PRTR officially missed data for SK in 2018, and was incomplete for DE and IT. Therefore, we used the German database (Federal Environment Agency, 2021), and estimated the missing data elsewhere by the average emissions for the years 2015–2017. Similarly, the values for 2018 provided by ICPDR were also assumed for the years 2015–2017. According to SwissPRTR, no emissions were reported for the Swiss Inn valley (Federal Office of the Environment, 2021).

Due to inconsistent names and places, double entries in the two E-PRTR databases were manually removed. WWTPs (mainActivityCode 5.f) were excluded from all databases. We intersected the industrial dischargers and the AUs and corrected the assignments where the country differed. An implausibly extreme TP release in 2017 in a Hungarian AU was divided by 1000 (unit error?).

2.3.5 Total population and connection rates to waste-water collection and treatment

The annual population at the end of the year was derived from national statistics and the global GHS-POP grid for 2015 (Schiavina et al., 2019) to account for the spatial variability. Accordingly, we used the values of the next year where national statistics referred to the 1st of January. For each country and year, correction factors were applied to the AU population obtained from the global grid, implicitly assuming that the internal migration is not relevant (Figure 11).

MONERIS also considers how many of the inhabitants are connected to sewer systems (Figure 13), to WWTPs via sewers (Figure 14), to septic tanks transported to WWTP, and to decentralized treatment plants (DCTP). DCTPs can emit either directly to surface waters (via pipes & ditches or sewers) or to the soil. Regional statistics on connection rates to sewers and WWTPs were available for most countries (Table 7, Figure 12), typically at NUTS3 level. We derived the AU values as area-weighted means. In AT, connection rates to WWTPs were available at NUTS2 level. They were used to adjust the AU values from the STOBIMO project – similar to the previous model setup.

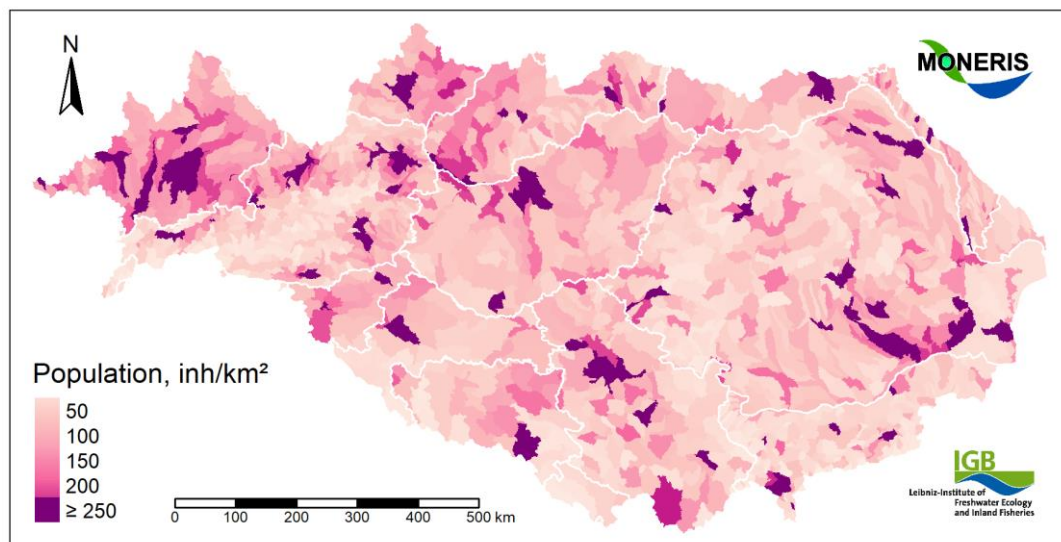


Figure 11. Mean total AU population, 2015–2018.

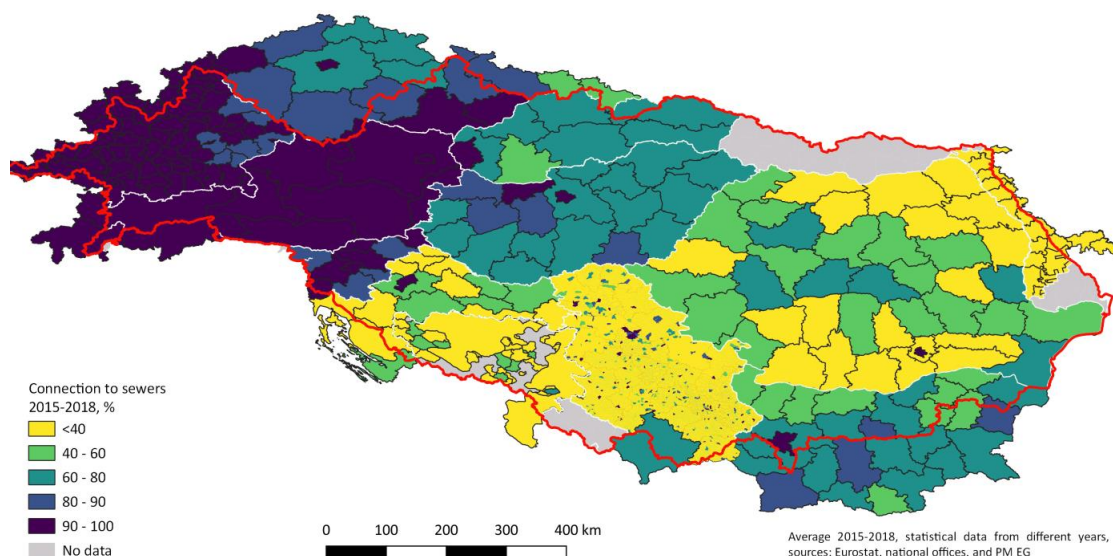


Figure 12. Connected population to sewer systems according the available regional statistical data, 2015–2018. Note the incomplete coverage of BA, and the missing data for UA and ME.

Statistical data for UA and ME were unavailable, and for BA incomplete. Here we relied on the agglomeration data of the UWWTD inventory. The connection rates to sewers and WWTPs for AUs the agglomerations fell into were estimated from the collection rate of loads (in p. e.). For each AU, the rate of loads collected by sewer systems (in %) and the rate of loads collected by sewer systems with WWTPs (connection type = ISCON, in %) were multiplied with the total generated load (in p. e.) and the three loads summarized. From these loads, the average collection rates were derived and multiplied with the total population. Given the approach, the estimated connection rates could be too high due to the missing agglomerations below 2000 p. e., or too low in AUs without assigned agglomerations. The loads of a few agglomerations in BA were assigned to multiple AUs (Table 6).

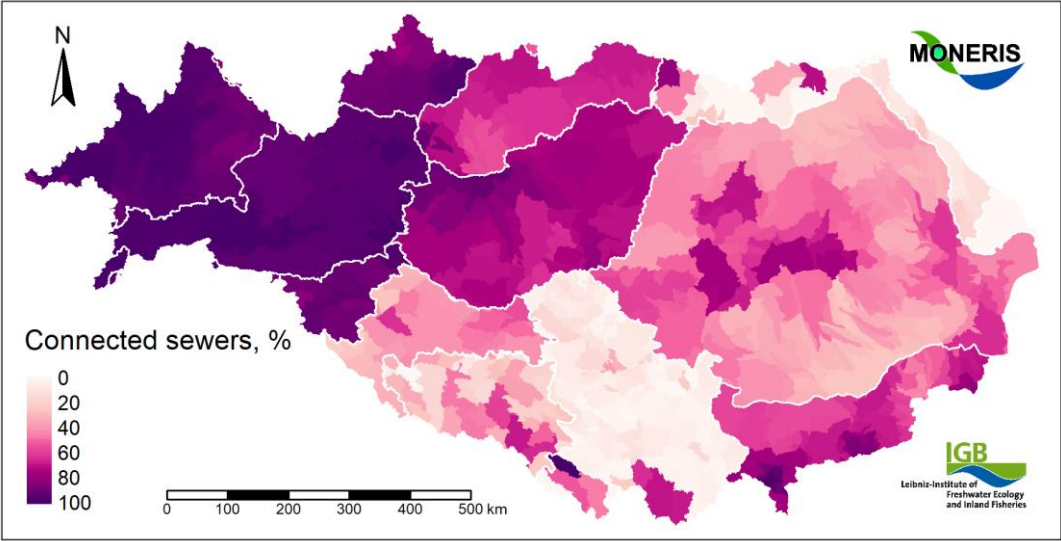


Figure 13. Mean connection rate to sewer systems of the population in AUs, 2015–2018. (Figure 11). The spatial variability in BA, ME, and UA might be affected by the use of the UWWTD inventory instead of statistical data. In MONERIS, inhabitants not connected to sewers use either septic tanks or decentralized treatment plants.

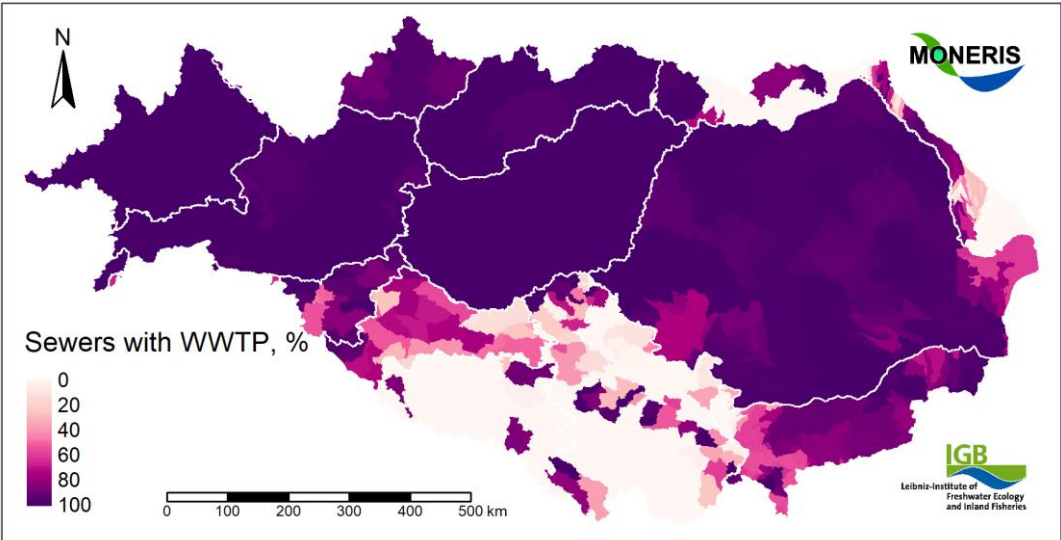


Figure 14. Ratio of connection rates to WWTPs and sewer systems (Figure 13), 2015–2018.

Table 6. List of agglomerations assigned to multiple analytical units.

Agglomeration	Assigned analytical units
BA_RS_Foca	606, 622
BA_RS_Han Pijesak	605, 623
BA_AG_BA_U1068	603, 605
BA_AG_U0034	633, 680
BA_RS_Laktasi	607, 652

Table 7. Overview of the available regional data. If not provided, septic tanks and DCTP were estimated from the population not connected to sewer systems (percent values). If not specified, the DCTP type will be derived from hydrogeology.

Country	WWTP	sewer	septic tank	DCTP	Comment
AT	x	x	100%	-	from STOBIMO adjusted to connection rates at NUTS2 level (2014–18) (Federal Ministry of Agriculture, 2020)
BA	-	(x)	-	100%	incomplete, from UWWTD inventory
BG	x	x	-	100%, soil	https://www.nsi.bg
CZ	x	x	-	100%	https://www.czso.cz
DE	x	x	x	(water, soil)	Regional statistics: DE-BY 2010, DE-BW 2016 + DCTP=septic=50% not conn.; DCTP 20% soil, 80% water (U. Kaul)
HR	x	x	IAS	(rest)	
HU	x	x	100%	-	
MD	x	x	IAS	(rest, soil)	
RO	x	x	90 % IAS	(water, soil)	DCTP: 10% IAS water, rest “dry sanitation” as in RS (C. Boscornea, 18.5.21)
RS	x	x	x	(rest, soil)	DCTP = “dry sanitation” as remainder
Kosovo	x	x			from Eurostat, merged with RS
SI	x	x	x	(rest)	
SK	x	x	x	(water, soil)	DCTP 10% water, 90% soil (E. Rajczykova, 14.5.21)
UA	-	-	0%	100%, soil	septic tanks expensive (N. Osadcha, 19.3.21)

In MONERIS, all inhabitants not connected to sewers are either connected to septic tanks or DCTP or septic tanks emptied into WWTPs, i.e. total pop = pop connected to sewers + pop connected to septic tanks + pop connected to DCTPs. All “IAS” in the regional statistics provided by the countries were considered as “septic tanks” which partly differ from previous assumptions. In case of DE-BY, however, this contradicted the official statistics used for the last setup which showed connection rates to DCTP of 90% for 2010. For other countries, we assessed the relevance of septic tanks and DCTPs from

national statistics (Eurostat, 2021b). Values for single years were assumed to be representative for the whole reference period.

Data on DCTP types was virtually inexistent, so our assumptions relied on the feedback received from the countries. If the DCTP type was left unspecified (“unknown”), MONERIS estimated the share of DCTP types according to the hydro-geology. The distribution among septic tanks and the different DCTP types changed noticeably e.g. in Serbia, where we considered “dry sanitation” as DCTPs with soil infiltration instead of the previous “unknown” (Figure 15). Soil infiltration resulted in high, though not complete retention as in isolated septic tanks. In addition to these assumptions, the modelling could not reflect the variety of technical solutions for independent waste-water collection and treatment and their efficiencies in retaining nutrient. Therefore, a large uncertainty in the model estimates remained.

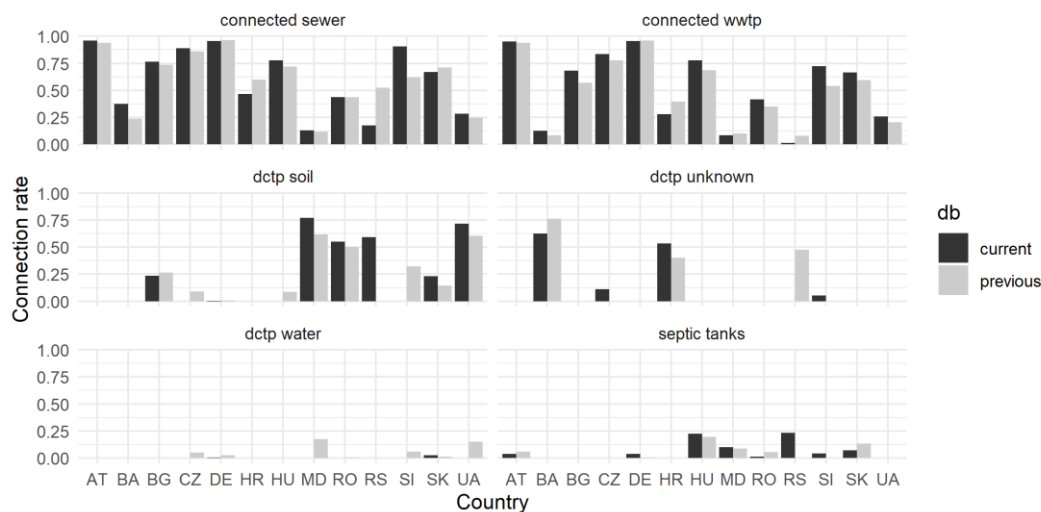


Figure 15. Connection rates to sewers, WWTP, and independent treatment within the DRB, 2015–18 (current) and 2009–2012 (previous database) relative to the total population.

2.3.6 Soil erosion

Outside Alpine areas, MONERIS requires soil-loss rates for arable land (separated by slope), grass land, and naturally covered (forested) areas. Soil loss rates have to be estimated with the commonly used universal soil loss equation (USLE), or one of its variants. Despite its age and its conceptual flaws, the empirical USLE remains the most popular modelling approaches, especially for large-scales applications (Borrelli et al., 2021). At large scales, the USLE factors have to be estimated, and various approaches exist for this purpose. As a consequence, soil-loss estimates from different data sources can vary considerably.

The previous MONERIS applications relied on a USLE-based map developed at IGB which applied e.g. simple relationships to estimate its R (rainfall erosivity) and K (soil erodibility) factors. Meanwhile, maps for EU-wide and global soil-loss assessments were published (Panagos et al., 2015, Borrelli et al., 2017) using a broader set of input data. These estimations cannot be seen as “realistic” due to the intrinsic limitations of the empirical USLE and the input datasets but may provide more consistency with other large-scale assessments. Given their different scales, the two maps do not share a common database. Furthermore, the EU map was provided at much higher resolution than the global map (Figure 16). Unlike the global map, the EU map considered soil management (conservation, USLE P factor). Therefore, data on tillage practice and crop rotation for soil conservation was not used for EU countries. For non-EU countries, we used the data provided for the previous DRBMP.

These soil-loss maps represent long-term average conditions. The reference periods of their R factors differed from the reference period for MONERIS. We estimated that the period 1982–2002 is most representative for their heterogeneous rainfall database and applied the rainfall change between 1982–2002 and 2015–2018 according to the European dataset (Cornes et al., 2018, ECA&D, 2021) to the current average rainfall (R) in AUs (partly derived from national datasets) – in line with the MONERIS approach to adjust the soil loss to the year or period of interest:

$$R_{ref_soilloss} = R_{AU,2015-18} R_{EOBS,1982-2002} / R_{EOBS,2015-2018}$$

The USLE does not consider gully erosion which is a key challenge in agricultural areas around the world (Vanmaercke et al., 2021). As large-scale quantitative maps on erosion rates of gullies are unavailable, the soil loss and the nutrient emission via soil erosion may considerably be underestimated in countries like RO and HU (Kertész and Gergely, 2011, Ionita et al., 2021).

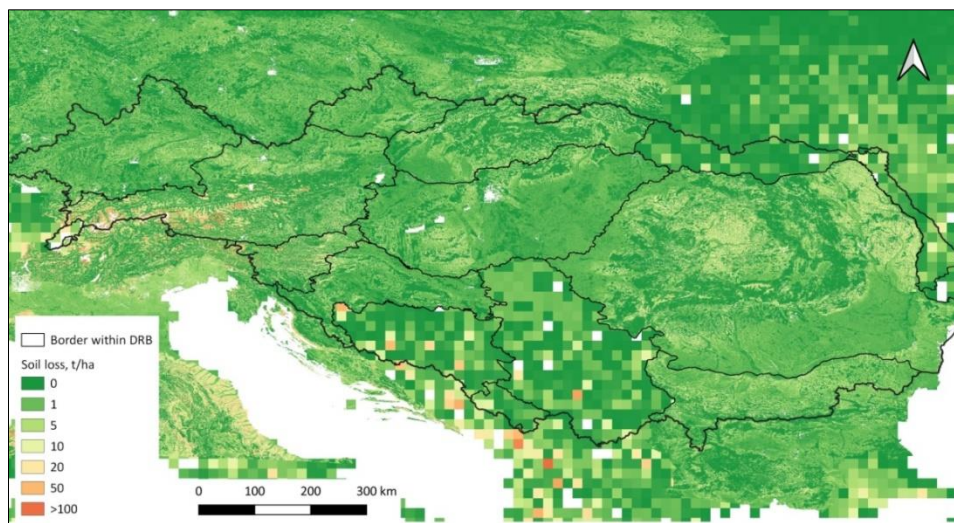


Figure 16. The two soil loss maps used for the MONERIS setup with missing data – cities, lakes, sea – in white. Note that the coarse global map in the background covers missing data in the detailed map for EU countries.

2.3.7 Further data updates compared to previous database

If not specified, the input data was provided by PM EG or NTG members.

- Land use and land cover

The Corine Land Cover 2018 (European Environment Agency, 2021a) was complemented by national maps for UA and MD. Their class values were translated to the MONERIS class values (Figure 17).

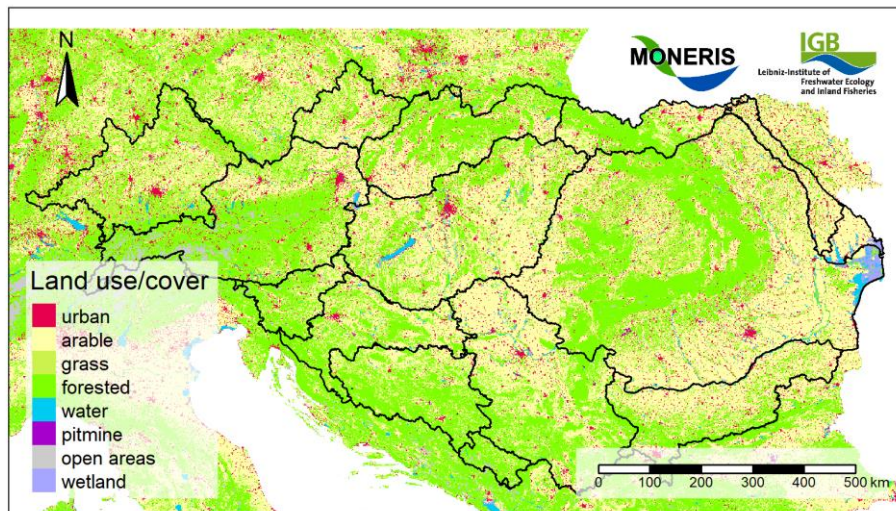


Figure 17. Land-use / cover classes as used by MONERIS.

- Tile drainage

New spatial data was provided by DE-BY, SK, and SI. The gridded potentially drained agricultural land for DE-BY was intersected with the agricultural used for MONERIS to calculate its share on all agricultural land. From the vector data for SK and SI (Ministry of Agriculture, 2019), we determined the drained area for each AU and the ratio to the agricultural land.

MONERIS calculates the emissions separately for arable and grassland and supports separate input values on the share of tile-drained areas and the N surplus. As only aggregated information for agricultural areas were available, we assumed the same input values for both land-use classes.

- Hydro-geology

A new version of the previously used European dataset (Federal Institute for Geosciences and Natural Resources and United Nations Educational, 2019) was combined with the national data from AT, HR, and SI for the last DRBMP. The hydro-geological classes were aggregated to the four MONERIS classes (unconsolidated & shallow / deep groundwater, consolidated & permeable / impermeable) following the previous approaches and their areas in each AU were determined (Figure 18).

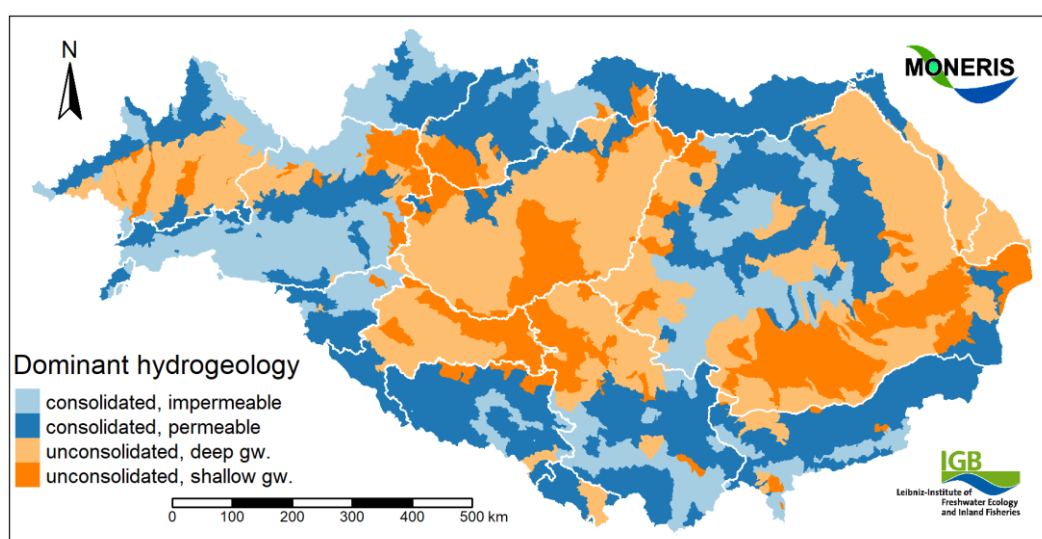


Figure 18. Dominant hydrological classes in AUs.

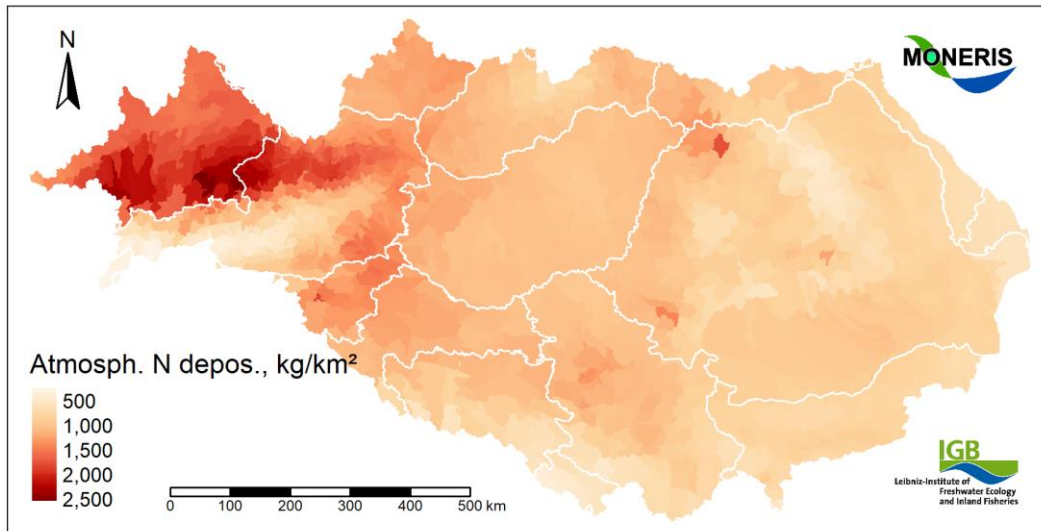


Figure 19. Mean atmospheric N deposition in AUs, 2015–2018.

For Germany, we used the HÜK250 and the HY1000 maps (Federal Institute for Geosciences and Natural Resources and German State Geological Surveys, 2019, Federal Institute for Geosciences and Natural Resources, 2019). Consolidated and unconsolidated rocks were identified according to the VF_bez attribute (Locker-, Festgestein). The permeability for consolidated rocks was derived from the “Lchar” attribute as “impermeable” if Lchar is “GWG”, or “permeable” otherwise. For unconsolidated rocks, the groundwater depth was estimated from the attribute “hygeo_name_en” of the HÜK1000: “shallow” if hygeo_name_en is “Extensive and highly productive aquifers”, or “deep” otherwise.

- Soil texture, clay and N content

We extracted the soil data from the MONERIS database for the EU MARS project (Lemm et al., 2021).

- Atmospheric deposition

We used an updated version of the EMEP dataset (Norwegian Meteorological Institute, 2019, Norwegian Meteorological Institute, 2020) to obtain the monthly and annual atmospheric emissions of NO_x and NH_y (in kg/km²) from the modelled dry and wet depositions of oxidized and reduced nitrogen (Figure 19). Values for the atmospheric P deposition were unavailable. So, the existing time-series was extrapolated.

- Precipitation

Similar to the previous model application, we replaced the European dataset (Cornes et al., 2018, ECA&D, 2021) with national datasets for AT (ZAMG, SPARTACUS dataset), DE (DWD, REGNIE dataset), HU, and SI. The mean monthly and annual precipitation was derived for each AU from these gridded datasets (Figure 20).

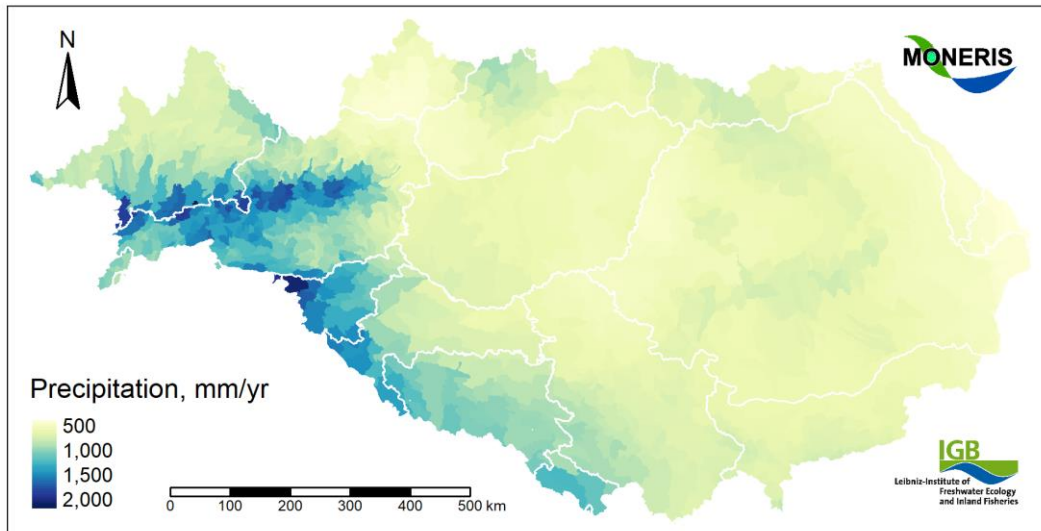


Figure 20. Mean annual precipitation in AUs, 2015–2018.

- Global radiation

The dataset (Cornes et al., 2018, ECA&D, 2021) was consistent with precipitation and air temperature. We derived the average monthly and annual global radiation (in W/m^2) at AU level.

- Water temperature

The monthly water temperature was derived from the air temperature using the regression models derived for the last MONERIS application. The new version of the gridded air temperature (Cornes et al., 2018, ECA&D, 2021) was consistent with new precipitation and air global radiation.

- P accumulation

We extended the existing multi-decadal time-series of P accumulation with national P balances from Eurostat (Eurostat, 2021a). The year 2018 was mostly missing and we filled the gaps as average of the last 5 years. For non-EU countries, we chose neighboring time-series, i.e. RO for MD and UA as well as the average of HR and SI for RS, BA, and ME. Due to the accumulation, the choice how to estimate annual P balances has less impact on model results than the estimation of N balances.

- Share of combined sewer systems on total sewers system length

The share of combined sewer systems were changed based on expert knowledge and country data: RS (100%), RO (UWWTD data), and AT (SCHTURM project).

- Riparian buffers

We used the few country data on riparian buffers provided for the previous MONERIS applications. However, their retention capacities were increased based on the median of published values (Gericke et al., 2020) (Table 8). We re-applied the assumptions regarding the retention of nutrients in the Nitrate Vulnerable Zones (NVZ), i.e. 60% of the area along streams is covered with riparian buffers with an efficiency of 20% (assuming not well-established riparian buffers but abandoned land). For EU countries without the “whole-territory approach” (all AUs with 100% NVZ), we derived the area coverage of the recent NVZ (2016–2019) as provided by the European Commission via ICPDR.

We did not consider the previous ad-hoc assumption of high sediment retention in the forested riparian zones within the catchments of rivers Prut and (to a lesser degree) Drava.

Table 8. Retention capacity for different buffer widths derived from Gericke et al. (2020). The values for dissolved nutrients were applied to the surface-runoff pathway, the values for particulate nutrients to the erosion pathway.

Buffer widths	Dissolved nutrients	Particulate nutrients
2–5m	55	75
5–10m	60	88

2.4 Observation data

The modelled loads were compared to loads calculated according to the TNMN approach. During the establishment of the AU network, these stations were already assigned to AU. In October 2020, we asked for monitoring data for 183 pre-selected stations with area deviations <10% (132 of which <2%). The number of suitable stations was actually higher as e.g. national stations near TNMN stations were not considered.⁶ For some countries, however, station areas were often unavailable. To improve the coverage, 41 stations without areas were included in the data collection, implicitly assuming that their locations and the AU network were correct. While daily water discharge was widely available, water quality data was sampled bi-weekly at best. This was mostly the case for TNMN data.

For the load calculation, water-quantity and water quality-data station ids were paired and labeled with one out of 147 ids. These pairs were selected because a) the assigned AUs for the quantity and quality station were identical, the distances of the paired stations < 5 km, the catchment areas of the quantity stations deviated <5% from the AU catchment and <10% from the quality stations (was also <5% for the station matching the criteria). 16 pairs mostly with missing areas for the quality station were manually included. 6 stations were manually excluded: a) RO6–8 and UA2 at the different river arms in the Danube Delta, b) RO20 which is at the Danube not r. Olt, and c) the Duna Szigetköznél at Rajka which receives only a small part of the discharge. Multiple records could represent the same location (or AU) with measured data from different sources, e.g. if TNMN and national data were available or for stations at or near borders.

For each pair id, monthly and annual loads for the years 2015–2018 were calculated from at least 350 water-discharge values and TN or TP concentrations measured in each month and finally averaged. The countries were asked to confirm TP concentrations >1 mg/l and TN concentrations >10 mg/l. In a few cases, these high values could be corrected. The calculated loads of neighbored stations were compared to assess their uncertainty and used, with stricter criteria regarding the sampling frequency, to validate the modelled TN loads and to calibrate the in-stream retention of TP.

2.5 Scenario implementation

2.5.1 Baseline scenario

The Baseline scenario was calculated for the year 2027. The reference setup was changed for

- Replies from countries

ICPDR surveyed the countries on measures until 2027. Only 3 out of 7 replies could be implemented in MONERIS (Table 9). The other 4 questions (on modified crop rotation, reduced tillage, buffer strips, and green landscape elements) were answered with absolute numbers for 2027 without current values as reference. However, they were indirectly considered in the scenarios on soil loss and riparian buffers (see below). For the N balances, we applied fixed annual factors to the time-series to reach the

⁶ This underlined that the established AU network is plausible and possible errors are rather local.

proposed reduction in 2027. The spatial pattern was not changed. This resulted in slightly lower N balances in the DRB (Figure 21 left). The P accumulation in soil increased with 1 kg/ha/yr.

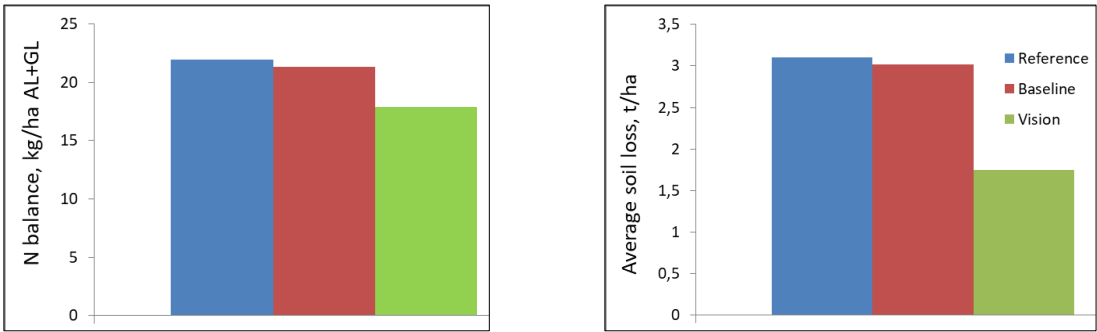


Figure 21. The scenarios address the N balances on agricultural land (left) and the soil-loss rates on arable land.

Table 9. Changes in the model database for the year 2027, without zeros (no change) and measures against soil loss.

Measure	Countries	Changes in 2027, %
N balance	AT, CZ, DE	-15, -15, -30
Tile-drained areas	UA	2
Construction of retention ponds in tile-drained areas	-	-

- Reduction of soil loss on steep slopes

Arable land on steep slopes is prone to soil loss. 5% reduction of soil loss from arable land on steep slopes (>8 %) was assumed resulting in a moderate reduction of total soil loss (Figure 21 right). The assumption replaced the replies of a few countries on modified crop rotation and tillage practices.

- More riparian buffers in NVZ

For EU countries, the area coverage of riparian buffers within NVZ was set to 100%. For non-EU countries, we assumed a whole-territory approach for NVZ with 10% acting as riparian buffers.

- No P-rich detergents

For all countries, the person-specific emission was set to 1.5 g/day (Figure 22).

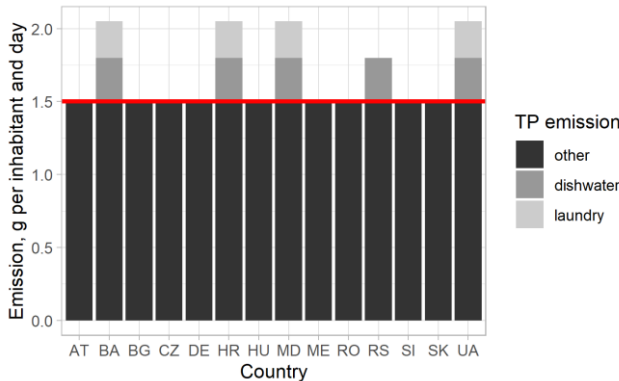


Figure 22. The scenarios assumed no TP emissions from dishwater and laundry (red line).

- More waste-water collection and treatment

Unlike the reference setup, the ICPDR scenario for the waste-water collection and the nutrient emissions were only derived for agglomerations >2000 p. e. For The assumptions for EU countries were

that all emissions (in p. e.) are either collected by sewer systems or by IAS (septic tanks or DCTPs). All waste-water collected by sewer systems is treated by WWTPs. Apart from agglomerations in EU countries, the nutrient emissions of 28 agglomerations in MD, RS, and UA were also changed. The increase in waste-water collection resulted in higher nutrient loads emitted by WWTPs (Figure 23).

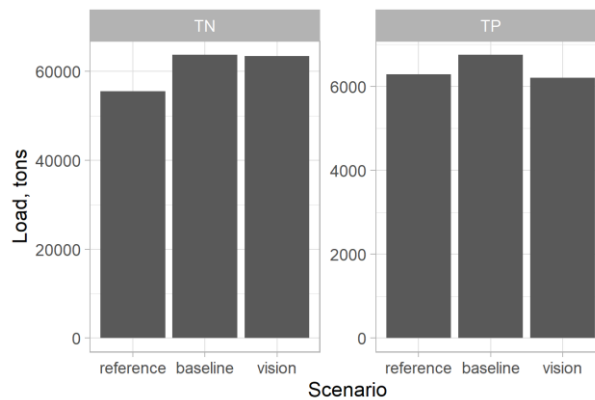


Figure 23. Nutrient loads in the WWTP inventory of MONERIS for the reference situation and the scenarios.

As agglomerations could have multiple DPs with different connection types (i.e. ISCON or NOTCON) and be located in (different) AUs other than the agglomerations, and DPs could belong to multiple agglomerations in different AUs, the workflow to modify the reference WWTP inventory consisted of

1. Aggregate water volumes, generated loads (in p. e.), TN and TP loads of DPs belonging to the same agglomeration and AU
2. Assign agglomeration to the dominant AU according to water volume, generated load, TN and TP load
 - a. Manual assignment for two agglomerations without dominant AU
3. Replace DPs in WWTP inventory with agglomerations if the nutrient load changed to the reference period
 - a. Calculate TN and TP concentration from load and water volume
 - b. Set zero water volumes to arbitrary value of 10^6 m^3 to avoid “loss” of nutrient loads⁷
 - c. Keep the two DPs which also belong to unchanged but larger agglomerations
 - d. Countries without DCTP (AT, HU) +DE: consider all loads in the WWTP inventory
 - e. Countries without septic tanks (BA, BG, CZ, HR, ME, UA) + MD+UA: consider only loads collected by sewers (i.e. the share of sewers on the collected loads)
 - f. For RS, SI, SK consider sewers + 30, 50, 20% of the IAS share

Note: Only 48 agglomerations had DPs in different AUs. ICPDR changed in some countries the IAS collection in the reference period to “not collected” in the scenarios. This was corrected.

Except for BA, ME, and UA, connection rates of the population for the reference period were obtained from statistical data. As the population and the spatial extent of agglomerations were unknown, we had to estimate changes in the connection rates from the changes in collection rates (Figure 24). For this purpose, we assigned the agglomerations to the AUs they fell into without taking into consideration their populations.

⁷ This issue is irrelevant for the reference situation as DPs with zero water volume also had zero nutrient loads.

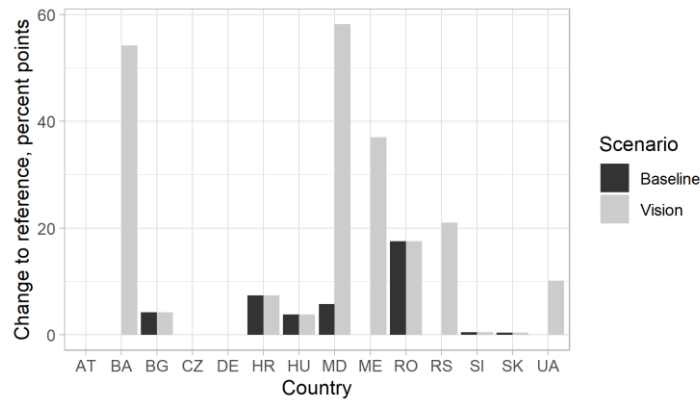


Figure 24. Collection rates in agglomerations >2000 p. e. compared to the reference period.

The workflow consisted here of these steps

1. Spatially intersect agglomerations and AUs
2. Aggregate the collection rates at AU level by weighting the generated loads
3. Set connection rate to collection rate if the latter changes significantly (≥ 10 percent points) and the connection rate is lower than the collection rate
4. Change connection rates to WWTP to connection rates to sewer systems for AUs in EU countries and in MD (where connection rates to sewers were changed)
5. Keep the ratios of septic tanks and DCTPs for the population not connected to sewer systems

In this way, the connection rates to sewer systems were changed for 294 out of 953 AUs in BG (31), HR (5), HU (7), MD (6), RO (242), and SK (3).

2.5.2 Vision I scenario

The Vision scenario was calculated for the year 2068 to avoid that past N balances affect the emissions. The Baseline scenario was modified and extended by

- More effective fertilization (lower N surplus)

The scenario adopted the “Farm to Fork” strategy of the EU which aims at reducing nutrient losses from fertilizers in the EU by at least 50%. We applied this reduction goal to the current average net N balance of the EU-27 (Eurostat, 2021a). As N balances vary from year to year, we considered the average of 2009–2014, i.e. the 5 most recent available values. This approach did not take into account that Eurostat balances for the reference period may differ from the regional N balances.

Like the regional values, the balances were corrected for the area difference between the agricultural land in MONERIS and in the official statistics. As agriculture only partly contributes to the atmospheric N deposition, we excluded this term. The N balance in all AUs was set to 7.5 kg/ha + current atmospheric N deposition. The time-series at national level was extrapolated from 2027 (Baseline) to 2068. As a consequence, the N balance increased in AUs with currently lower values.

- More erosion control (towards a tolerable soil loss)

Soil-loss rates E on arable land were halved up to the threshold of 1 t/ha:

$$E_{Vision} = \max(0.5 E_{ref}, 1)$$

Using a relative reduction instead of a fixed threshold took into account that soil-loss rates depend on site characteristics. The chosen threshold was considered as tolerable, sustainable soil-loss rate in

Europe (Verheijen et al., 2009). Due to its multiplicative character, a reduction of 50% can be achieved by reducing the C, L, or P factors of the USLE accordingly, e.g. by changing tillage practices, crop rotation (less maize), mulching, and intercropping.

- More effective waste-water treatment in non-EU countries

Similar to the Baseline scenario, ICPDR provided nutrient emissions from agglomerations which we assigned to the dominant AUs of their DPs. Connection rates were also changed if the collection rates substantially changed. The rules for EU countries in the Baseline scenario (all waste-water collected by sewer systems or IAS, and is treated in WWTP if collected by sewer systems) were applied to non-EU countries. The connection rates to sewer systems were changed for 100 out of 201 AUs in MD (23) and RS (77), in addition to BA, ME, and UA.

- More riparian buffers in non-EU countries

For non-EU countries, the area-coverage of riparian buffers in NVZ was set to 100%.

2.5.3 Vision II and III scenarios

Vision I was further adapted to

- More efficient NVZ to retain emissions (via surface runoff and soil erosion, Vision II)

The efficiency of the NVZ was doubled, i.e. changed from 20% to 40%. Changes in real riparian buffers were not addressed.

- Hydrological changes (Vision III)

The average hydrology was replaced with the water discharge and precipitation of the wettest and driest years. Using the European precipitation dataset and modelled (and adjusted) discharge, we identified 2003 and 2011 as years with the lowest precipitation and discharge, and 2010 with the highest values for the whole DRB (Table 10). This might differ among sub-catchments and countries. The years 2003 and 2011 were averaged. To account for the four national precipitation datasets, we calculated monthly ratios to 2015–2018 and applied them to the AU values for the reference period.

Precipitation changes (e.g. more dry spells) can also affect plant growth and in turn soil cover (soil erosion) and N balances. Likewise, future rainfall might become more or less erosive, independent of the total precipitation. However, these effects were not considered, and the envisioned (low) soil erosion and N surplus were not modified.

Table 10. Indicators for the selection of dry and wet years, and the values (rank) for the selected years.

Indicator	Unit	2003	2010	2011	Average
Mean annual precipitation (2000–2019)	mm	539 (2)	892 (20)	522 (1)	702
Mean summer precipitation (2000–2019)	mm	345 (2)	550 (20)	357 (3)	420
Local water flux (2003–2013)	m ³ /s	6040 (2)	11162 (11)	6012 (1)	7710
Local water discharge (2003–2013)	m ³ /s	5731 (1)	10889 (11)	5842 (2)	7329

3 Model results

The tables with pathway- and source-specific MONERIS results at AU level were provided to ICPDR.

3.1 Spatial variability of nutrient emission

The modelled average basin-wide nutrient emissions⁸ to surface waters were 513 kt N/yr and 31 kt P/yr. This corresponds to area-specific emissions of 634 kg N/km²/yr and 38.4 kg P/km²/yr. The emissions were significantly lower than the results for the previous DRBMP which was expected after the revisions of the N balances and the WWTP inventory. Nonetheless, this decrease may partly reflect real improvements since 2012.

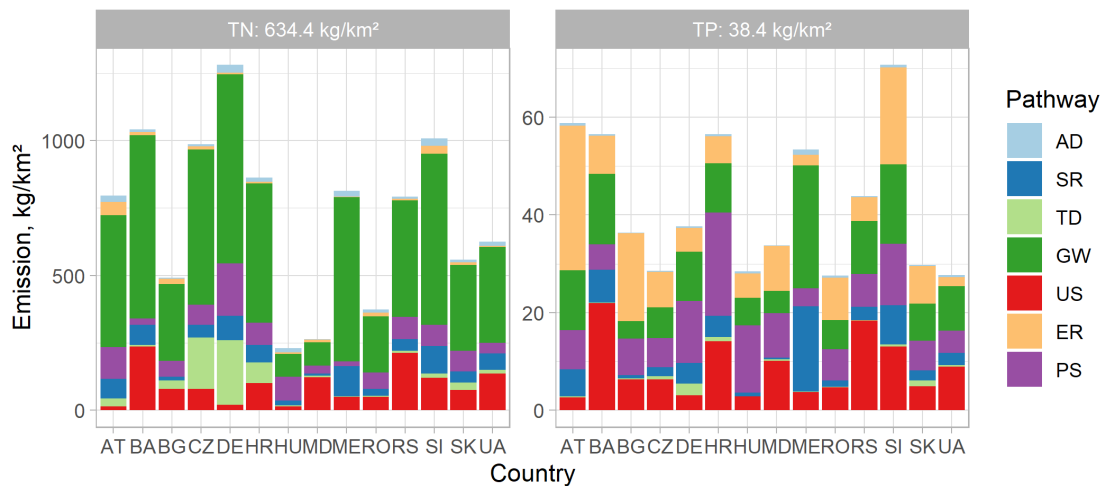


Figure 25. Variability of nutrient emission within the Danube River Basin, 2015–2018.

The area-specific values varied among the countries ranging from <300 (HU, MD) to 1300 kg N/km²/yr (DE) and from <28 (UA, RO) to 71 kg P/km²/yr (SI) (Figure 25). The spatial variability was even more pronounced for the land-use classes in MONERIS. The highest average area-specific emissions were associated with urban and open areas. These land-use classes only covered about 6% of the DRB which limited their overall contributions to the nutrient emission. Nonetheless, urban areas were important sources of nutrients besides agricultural land (Figure 26).

The contribution of the land-use classes varied with the natural settings (i.e. terrain, soils), the intensity of agriculture (i.e. fertilizer input) as well as the generation, collection, and treatment of waste-water. Accordingly, the emission from agricultural land was higher in erosion-prone areas as well as countries with high N surplus than elsewhere (Figures 27–28). An overview of the total and pathway-specific emission per country is given in Table A and Table B in the Appendix.

⁸ These aggregated total monthly emissions were also used for the load calculation and are the reference for this report. The model also calculates annual emissions with slightly different approaches. The shares of the pathways on these annual emissions were applied to the aggregated monthly total emissions. According to the first, the basin-wide emissions would be 500 kt N/yr and 31 kt P/yr.

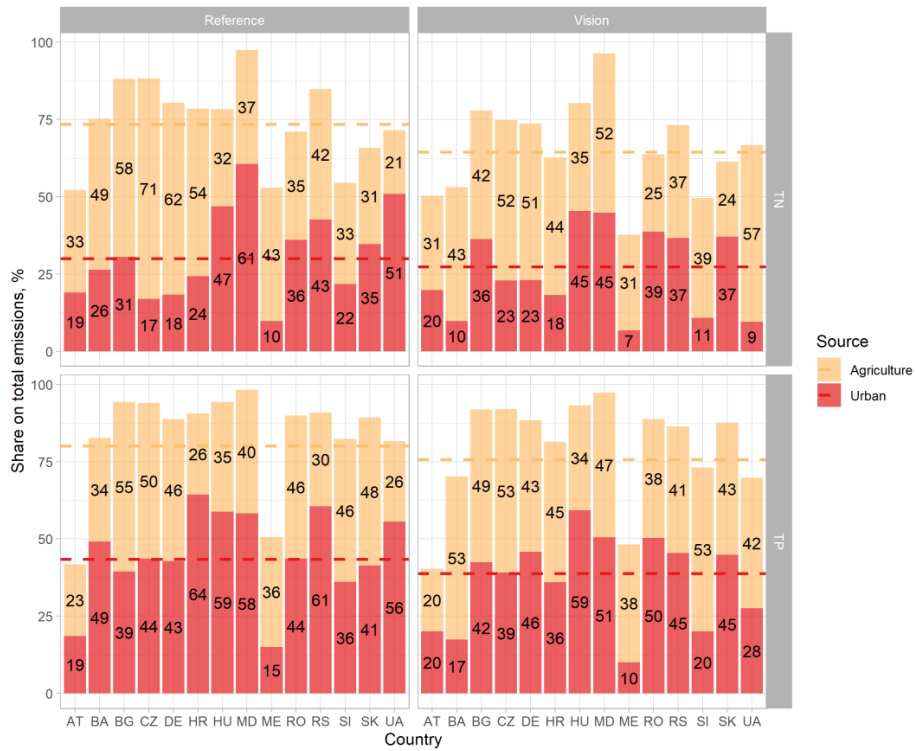


Figure 26. Share of agricultural land (arable land + grassland) and urban areas on total emissions of N (top) and P (bottom) for the reference period (left) and the Vision scenario (right). The values were derived from Figures 27–28. The stacked dashed lines show the basin-wide mean values.

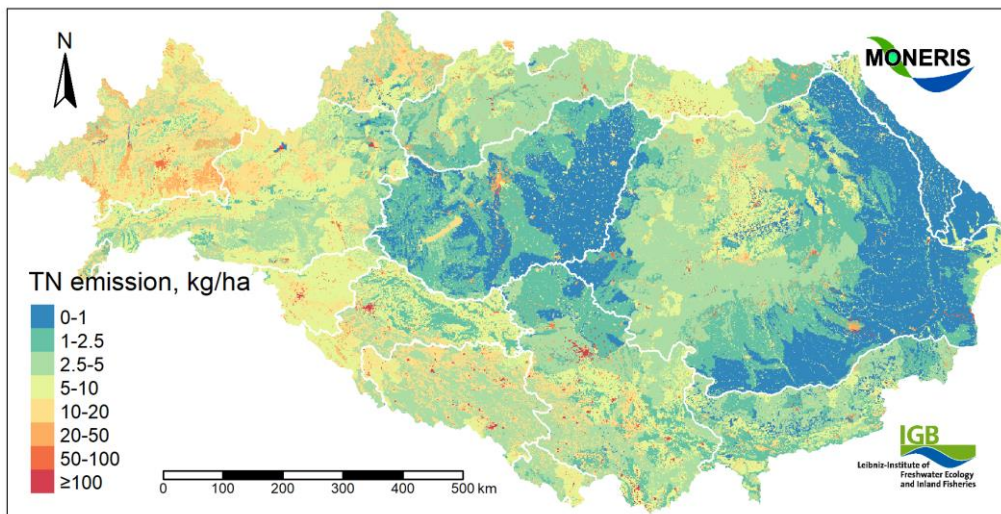


Figure 27. Mean N emission disaggregated by land use, 2015–2018. Artefacts may arise due to inconsistent input data (e.g. gridded population and urban areas) as well as point sources assigned to discharge points not agglomerations. Water area was taken from MONERIS not the land-use map.

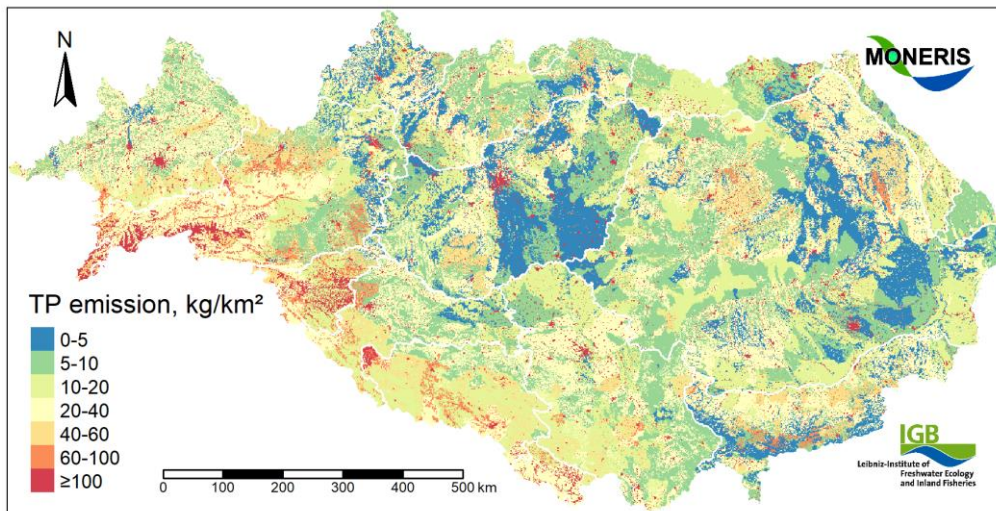


Figure 28. Mean P emission disaggregated by land use, 2015–2018. Artefacts may arise due to inconsistent input data (e.g. gridded population and urban areas) as well as point sources assigned to discharge points not agglomerations. Water area was taken from MONERIS not the land-use map.

3.2 Contribution of emission pathways⁹

Soil erosion was the most important pathway for P (soil erosion was far less relevant for N), with 50% contribution in the mountainous countries AT and BG. Urban systems were important for N and P in regions with high population but low connection rates to sewer systems such as in BA and in RS. N emissions via groundwater dominated in most countries (Figures 25–29).

The emission via diffuse pathways and some core model assumptions – in addition to the overview of recent model changes in section 2.1 – are briefly described below. Point sources are skipped because they just represent the inventory of WWTPs and industrial dischargers, and atmospheric depositions (on surface water) because of their low contributions. Venohr et al. (2011) and Lemm et al. (2021) provide more details about the modelling approaches. The area-specific emissions refer to the AU area to facilitate the comparison.

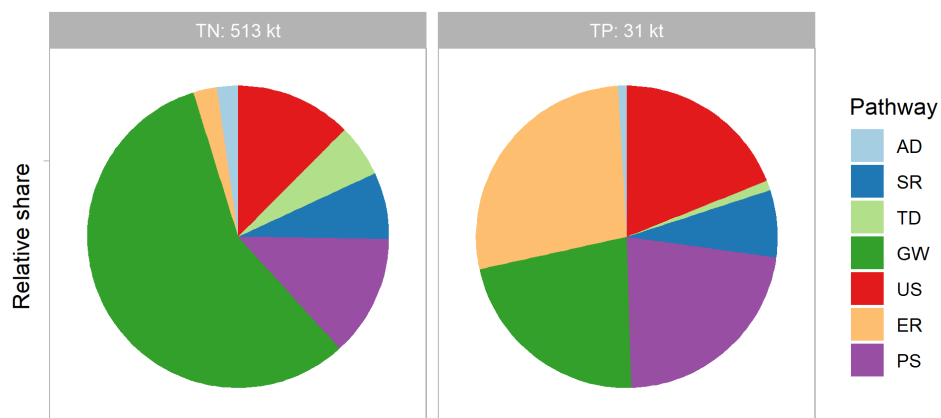


Figure 29. Mean contribution of pathways to the basin-wide nutrient emission, 2015–2018.

⁹ The pathways are henceforth abbreviated as AD (atmospheric deposition), SR (surface runoff), TD (tile drainage), GW (groundwater, i.e. subsurface flow), US (urban systems), ER (soil erosion), PS (point sources).

3.2.1.1 Emission via Surface runoff

Surface runoff was of equal relative importance for N and P emissions. The emissions (Figures 30-31) are derived from the nutrient concentration and the surface runoff (i.e. overland flow, Figure 32). WSP is a new model input (Figure 33) to estimate the P concentration in the surface runoff. However, the P content on soils is typically only available as plant-available P, if at all. As plants can emit acids to extract P adsorbed at soil particles, plant-available P is usually higher than WSP but may be converted to WSP using empirical relationships (cf. section 2.1). The N concentration originates from the atmospheric deposition. The surface runoff is derived from total runoff using an empirical relationship based on streamflow disaggregation (Carl and Behrendt, 2008, Carl et al., 2008).

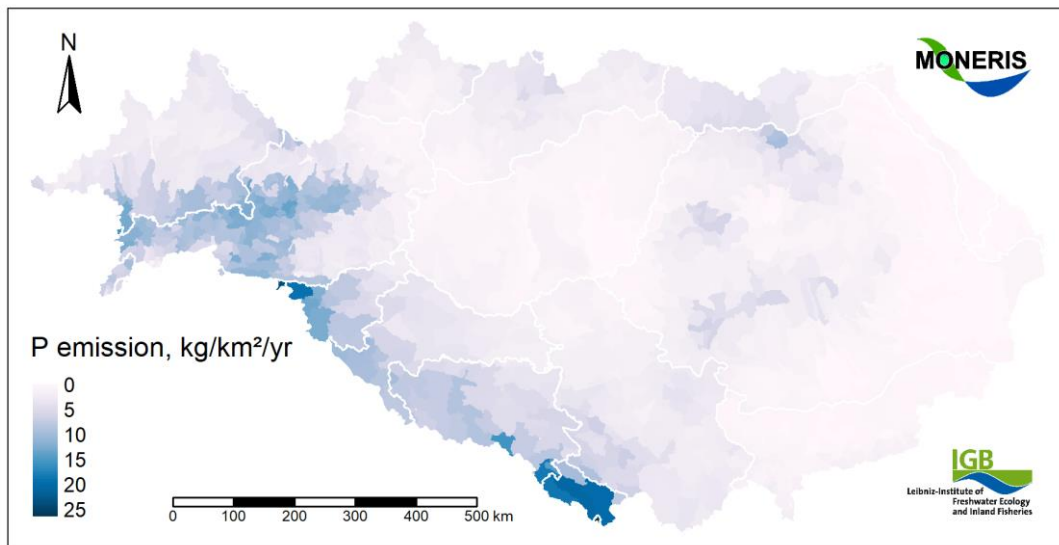


Figure 30. Mean P emission via surface runoff for AUs, 2015–2018.

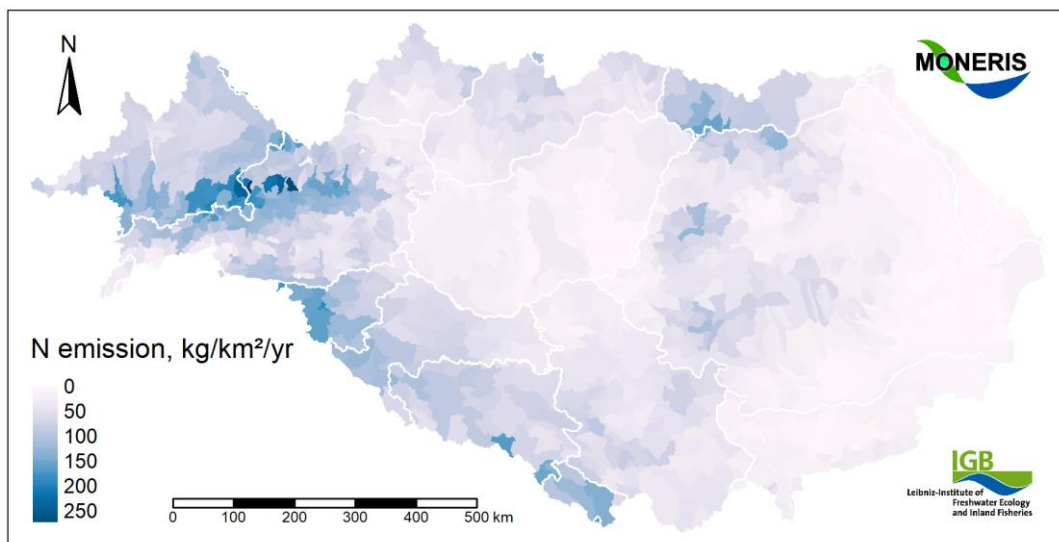


Figure 31. Mean N emission via surface runoff for AUs, 2015–2018.

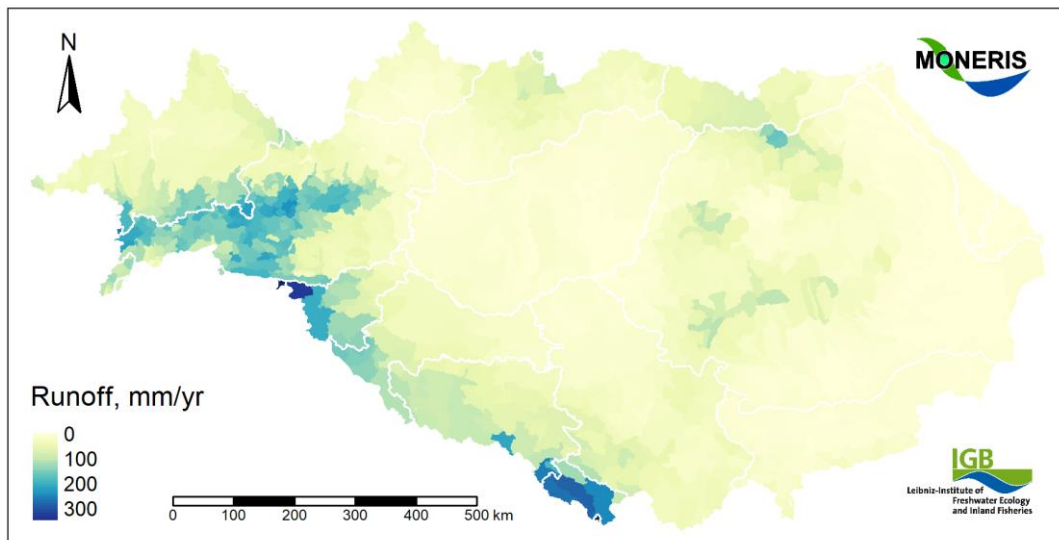


Figure 32. Mean surface runoff for AUs, 2015–2018.

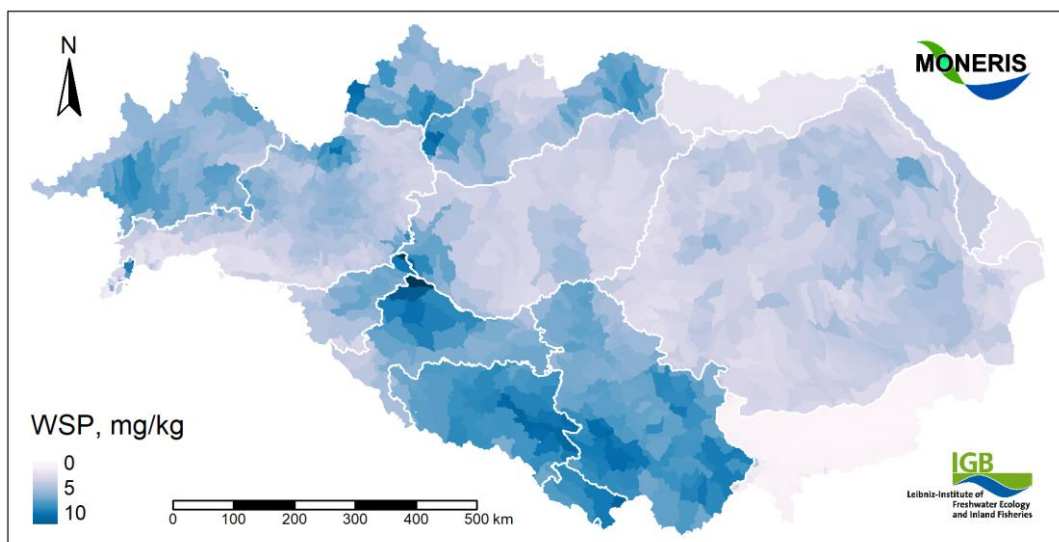


Figure 33. Mean water-soluble P in agricultural soils for AUs.

3.2.1.2 Emission via Tile drainage

The model considers the N surplus and the retention (fixation and denitrification) in the root zone. In contrast to arable land, a significant N fixation in the biomass can be expected for grassland (Heidecke et al., 2015). Consequently, the N loss under grassland is much higher than under arable land, which could also be shown in lower N concentrations (Hirt et al., 2011). The N emission via tile drainage (Figure 35) is calculated from the N concentration and the discharge via tile drainage (Figure 34). The latter is estimated with monthly precipitation-discharge ratios (Hirt et al., 2011). For the P emissions (Figure 36), soil-type specific concentrations are applied (Table 11).

Table 11. Considered TP concentrations in tile drainages for different soil types.

Soils type	TP concentration in mg/l	Soils type	TP concentration in mg/l
Sandy soils	0.2	Fens	0.3
Loamy/Silty soils	0.06	Bogs	2.0

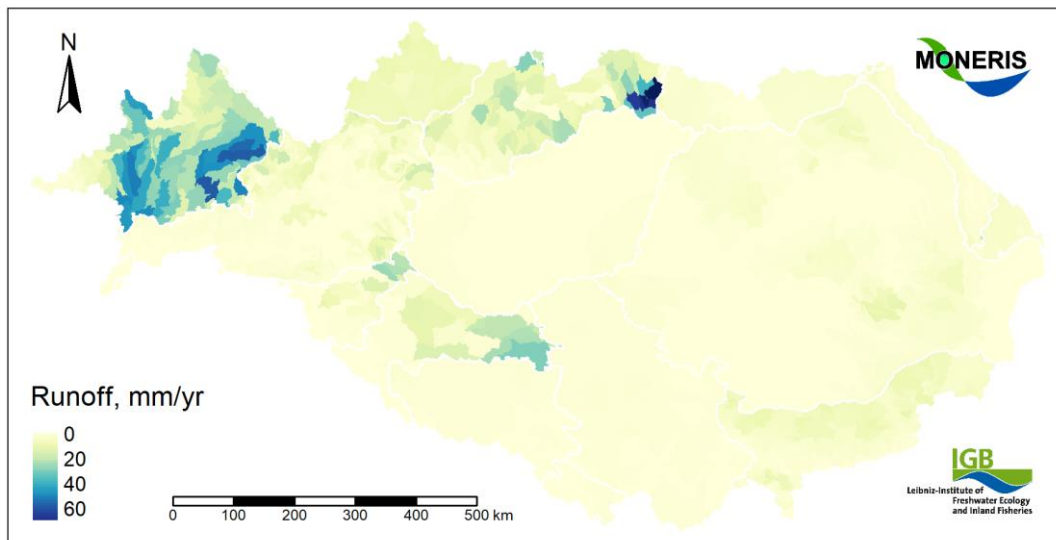


Figure 34. Mean annual discharge via tile drainages, 2015–2018.

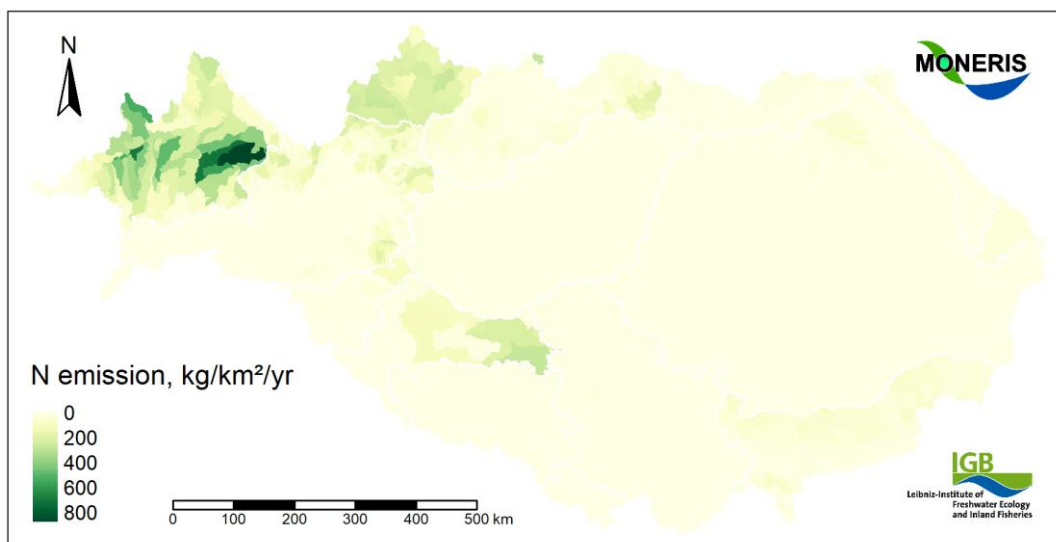


Figure 35. Mean N emission via tile drainages, 2015–2018.

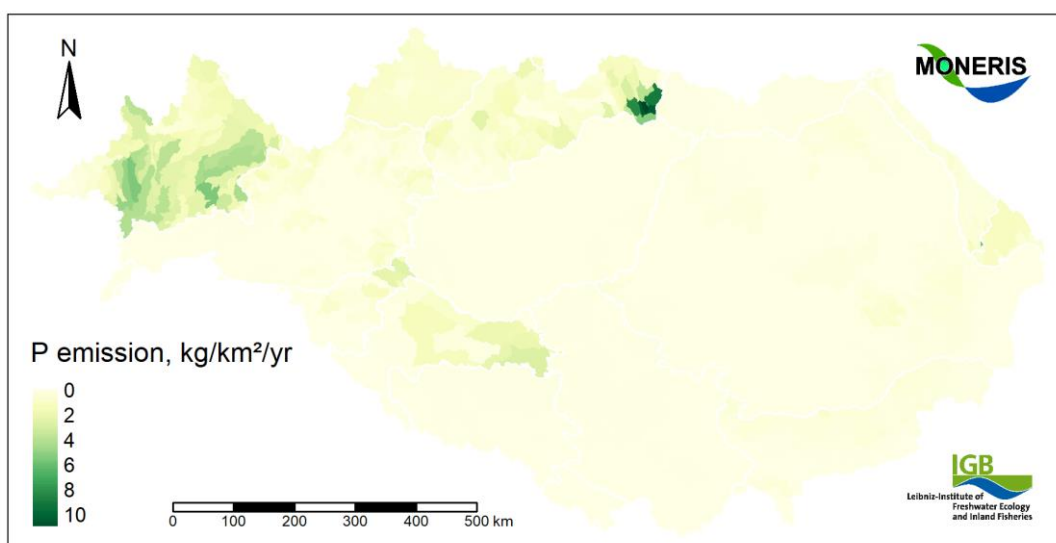


Figure 36. Mean P emission via tile drainages, 2015–2018.

3.2.1.3 Emission via Soil erosion

MONERIS relies on USLE estimates except for snow- and ice-covered in mountainous areas. For the emission via erosion, the estimates of the USLE maps (Figure 16) are corrected with an empirical sediment delivery ratio (SDR) – which accounts for sediment deposition along the pathway to the surface water –, the P content in soils which is derived from cumulated multi-decadal P balances, as well as an enrichment ratio as the relative P content in the sediment increases along the transport pathway. The AU-wide SDR is estimated from the average slope and the share of arable land.

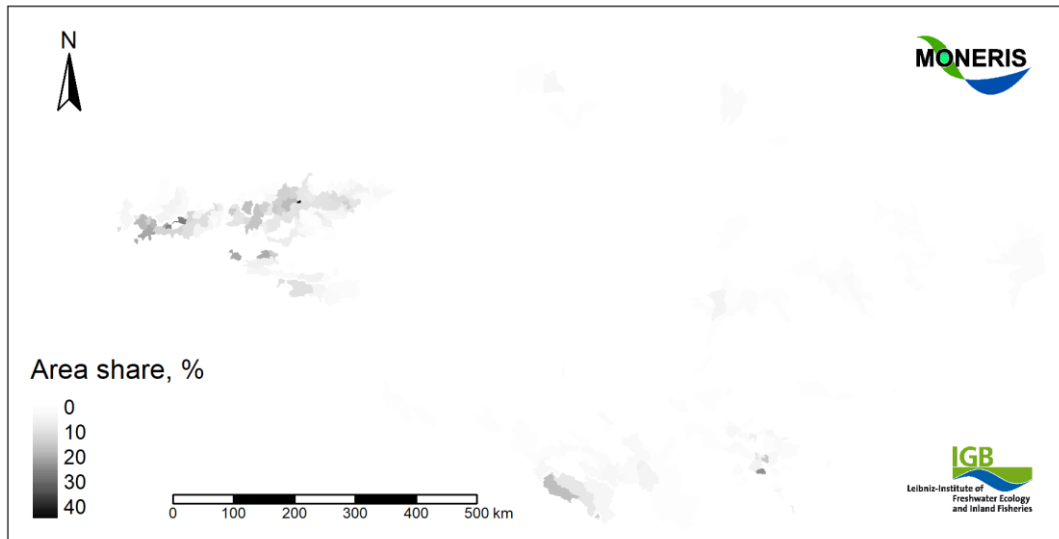


Figure 37. Share of open area on total AU area in %.

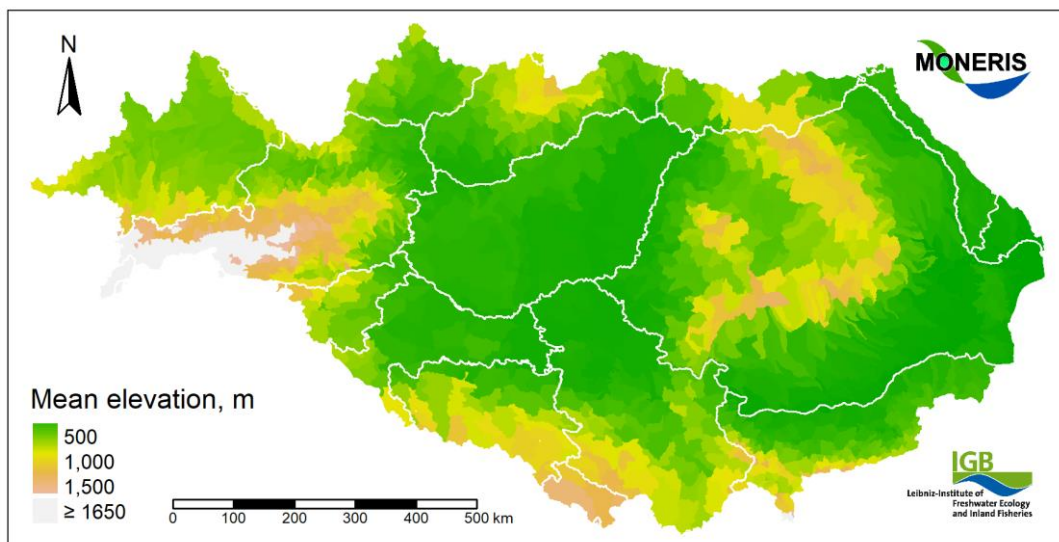


Figure 38. Mean AU elevation, elevation above which snow- and glacier melt is relevant in grey.

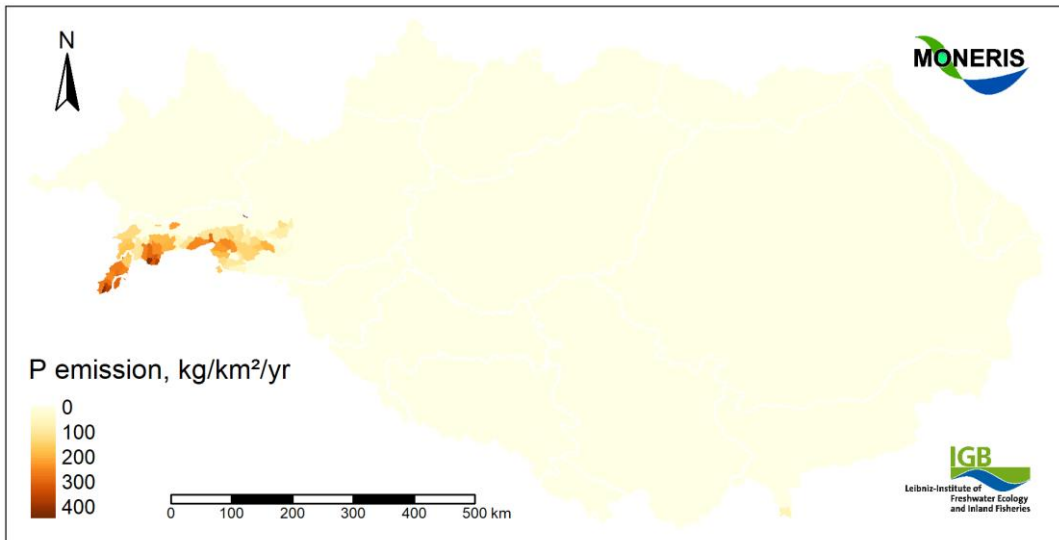


Figure 39. Mean area-specific TP emission via erosion from snow and ice covered areas, 2015–2018.

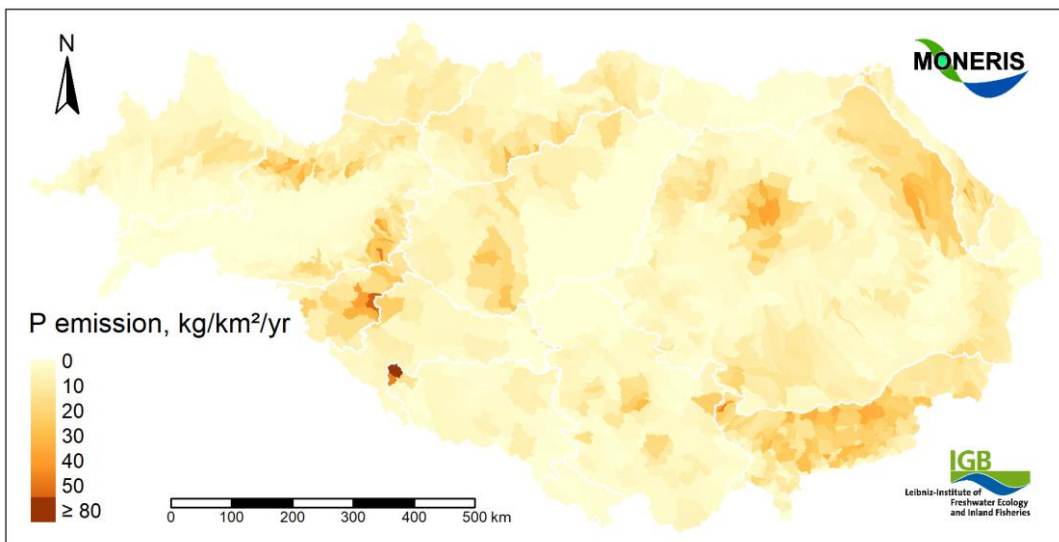


Figure 40. Mean area-specific TP emission via erosion from arable land, 2015–2018.

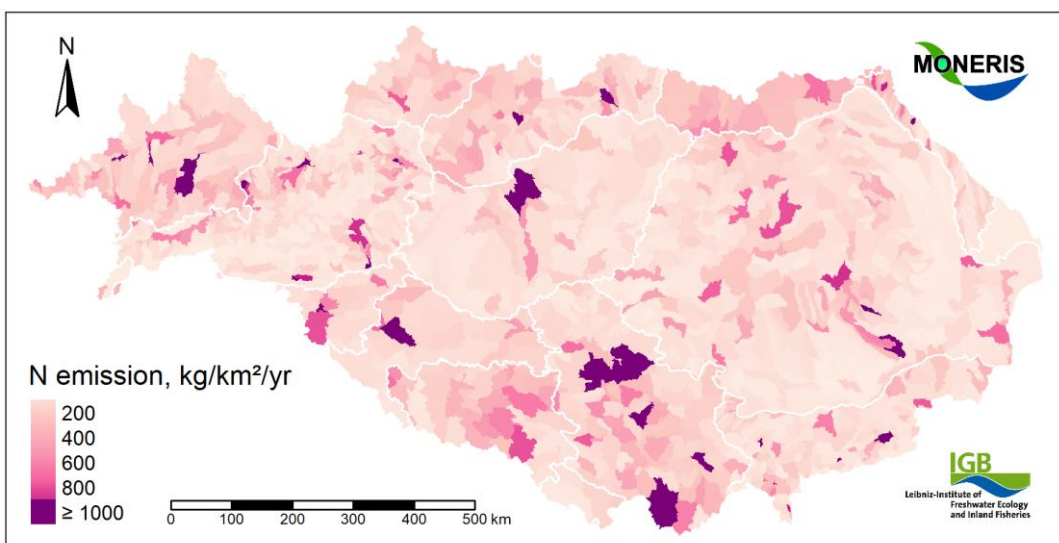


Figure 41. Mean N emission via urban systems for AUs, 2015–2018.

3.2.1.4 Emission via Urban systems

Urban systems comprise point sources (WWTPs and industrial dischargers) as well as sewer systems and decentralized treatment plants (DCTP). DCTPs are an inhomogeneous group of different treatment techniques of variable efficiency. Depending on legislative regulations and the historical development, DCTPs may be one-chamber sedimentation systems or even two-stage treatment systems. Furthermore, the treated effluents can either be discharged directly or indirectly (via a soil-groundwater passage with an additional retention) into surface waters. Figures 41 and 42 (as well as the disaggregated emissions) reveal the importance of (major) cities for the nutrient emissions.

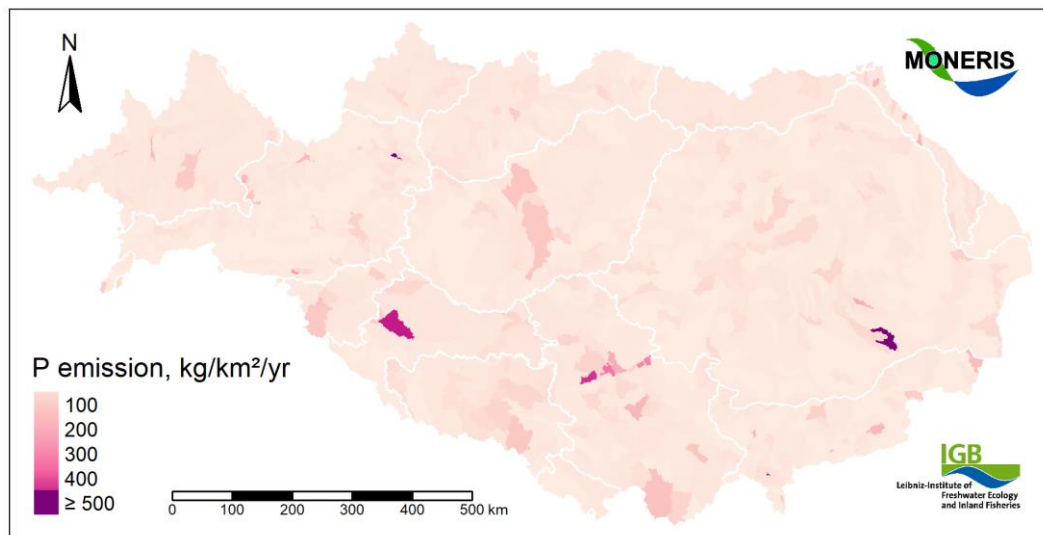


Figure 42. Mean P emission via urban systems for AUs, 2015–2018.

3.2.1.5 Emission via Groundwater

Groundwater (i.e. subsurface flow) was the dominant N pathway in the DRB – similar to previous results for the DRB and also for many other European river basins. MONERIS calculates the nutrient emission (Figures 46–47) from the groundwater discharge (Figure 43) and the mean N and P concentrations in the groundwater aquifer. The groundwater discharge is calculated as the residual of the total discharge without all other pathways because AU borders are not identical to aquifer borders. In absence of input data, the residence time is estimated from the long-term groundwater discharge.

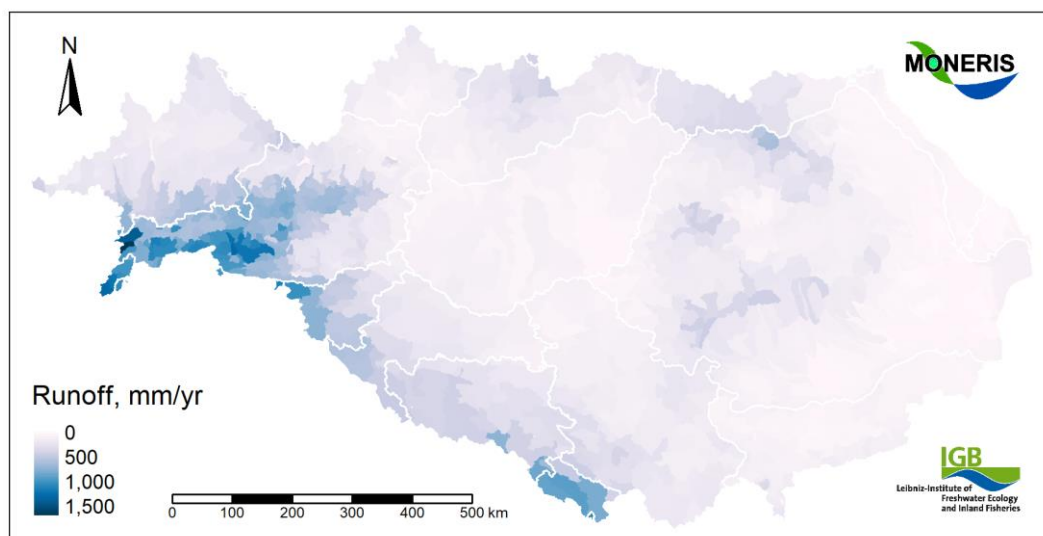


Figure 43. Mean groundwater runoff for AUs, 2015–2018.

The agricultural N surplus and its change during the residence time is the key factor for the N concentration. The concentration is further determined by the denitrification and fixation in the unsaturated zone in the soil and the leakage water. N concentrations in areas with low N surplus and low amounts of leakage water can exceed N concentrations in areas with high N surplus but high amounts of leakage water. The P concentration is derived from soil-specific values.

The subsequent retention in the aquifer is estimated from the geo-hydrological conditions (Figure 44). While the retention is low in consolidated rocks (compare Figures 44 and 45), it can be very high in unconsolidated rocks, especially if groundwater is shallow.

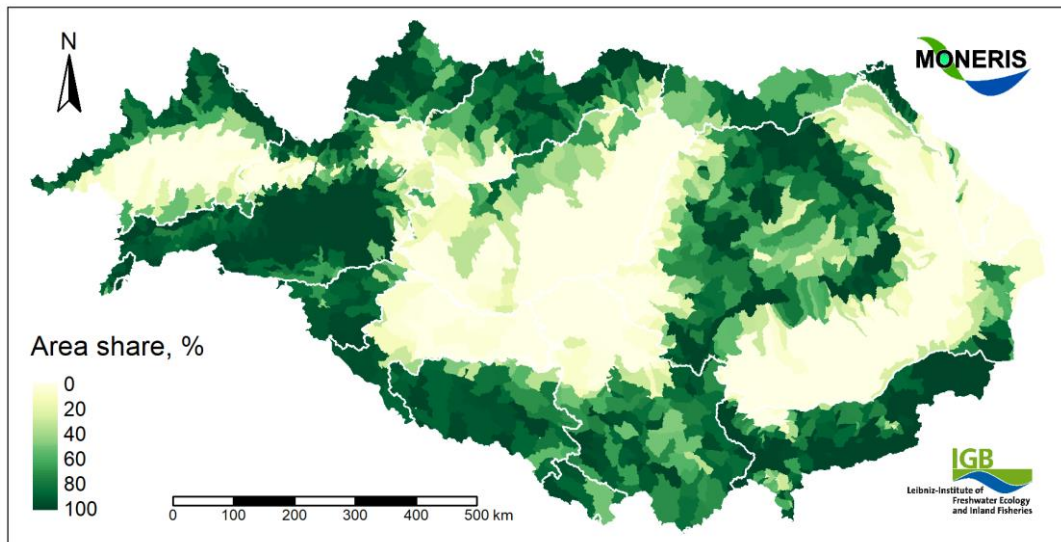


Figure 44. Share of consolidated rock on total AU area, 2015–2018.

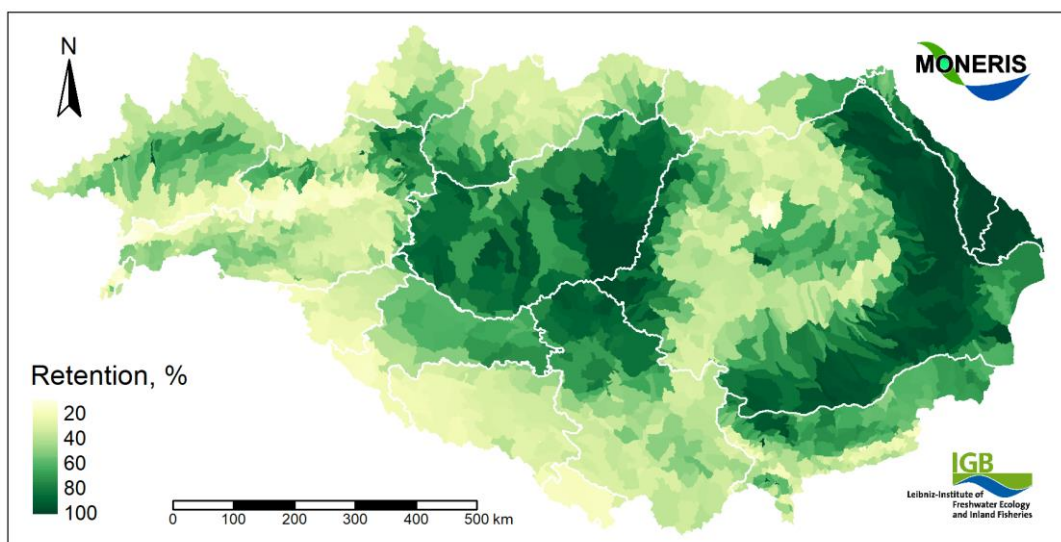


Figure 45. Mean N retention in the groundwater at AU level, 2015–2018.

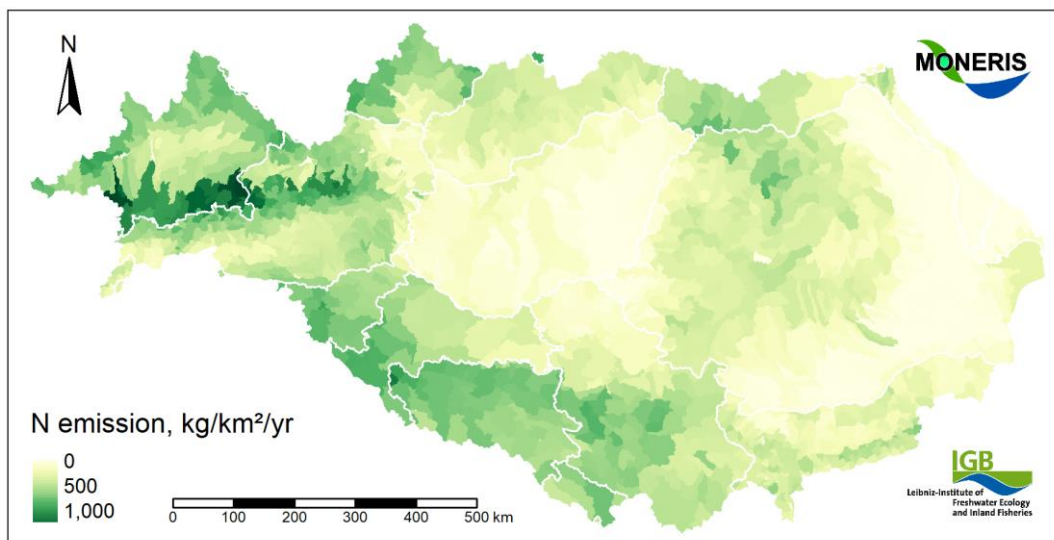


Figure 46. Mean N emission via groundwater for AUs, 2015–2018.

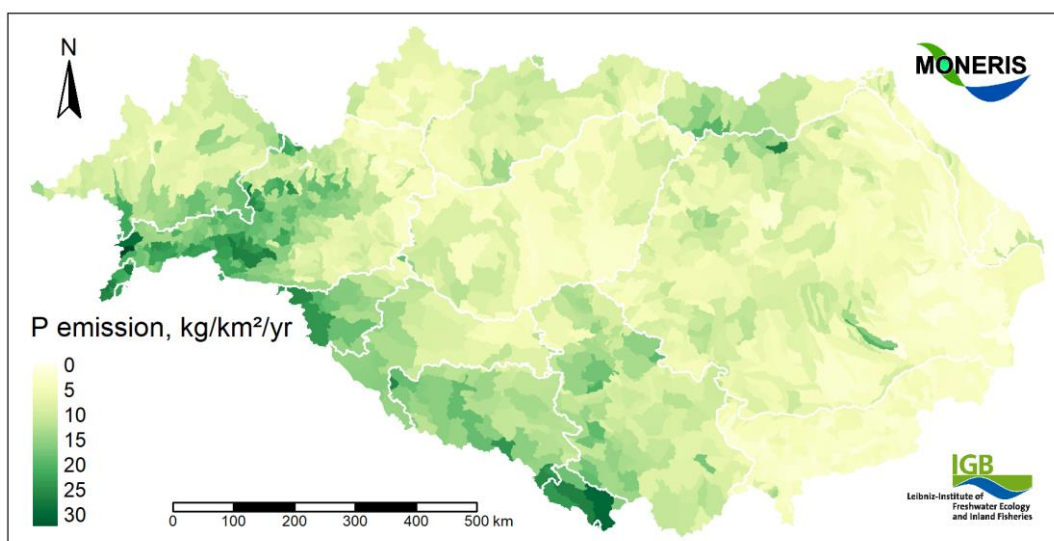


Figure 47. Mean P emission via groundwater for AUs, 2015–2018.

3.3 Nutrient load and load comparison

On average, 314 kt N/yr and 15.5 kt P/yr reached the Danube at Reni, located downstream the mouth of r. Prut, and 297 kt N/yr and 15.2 kt P/yr enter the Black Sea. The load underestimation of 10–15% can partly be explained with the underestimated discharge (-5%, Table 12). Additionally, the observed P load increased disproportionately downstream the Iron Gates for both increasing discharge and concentration (according to the TNMN database, not shown). A high in-stream remobilization seems to be likely but requires further investigation. The observed and modelled concentrations were close to the Black Sea targets of 0.09 mg P / l and 1.2 mg dissolved inorganic N / l.¹⁰

We selected 18 monitoring stations in 17 AUs for the validation of N loads and the calibration of P loads, mostly along the Danube (Figure 48). 13 average N loads were used for the model validation. They were selected if 3 out of 4 annual values could be calculated as even the stations with the lowest

¹⁰ The average (unweighted) DIN concentration at Reni was 1.22 mg/l for the years 2015–2018 which corresponds to 1.73 mg TP/l. The TP concentration was 0.095 mg/l.

average sampling frequencies was within an acceptable range of model deviation ($\bar{n} = 13.3$, TNMN station HU7, r. Drava).

Table 12. Discharge Q, load, and calculated (i.e. weighted) concentration c at Reni, r. Danube (TNMN code RO5). Observed Q from daily, modelled from monthly Q.

Parameter	Observation			Model		
	Q, m ³ /s	Load, kt	c, mg/l	Q, m ³ /s	Load, tons	c, mg/l
TN	6074	350	1.827	5780	314	1.722
TP	6074	18.0	0.094	5780	15.5	0.085

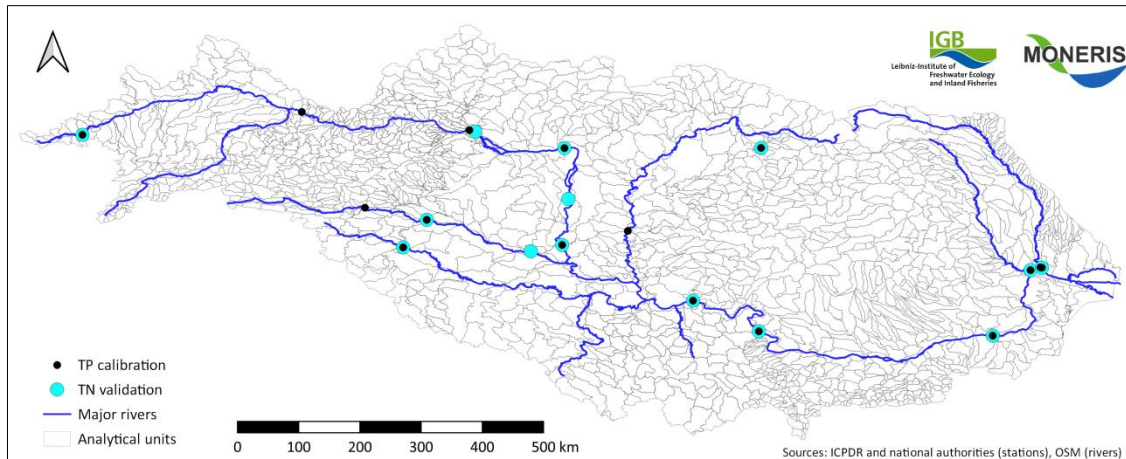


Figure 48. Stations for the calibration of the in-stream P retention (black) and the validation of N loads (blue).

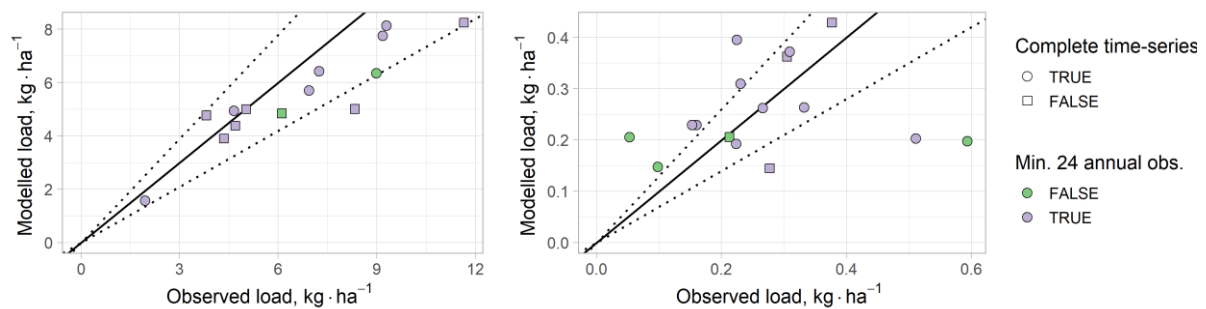


Figure 49. Comparison of modelled and observed TN (left) and TP area-specific loads (right). The largest deviations occurred at stations with incomplete time-series (3 out of 4 years, squares) and less than bi-weekly monitoring (in green).

Table 13. Model performance for N and P loads in tons. Ideal bias is 0%, r² and Nash-Sutcliffe efficiency 1.

Parameter	n	Bias, %	r ²	Nash-Sutcliffe efficiency
TN	14	-8.80	0.98	0.97
TP	16	5.70	0.90	0.89

Despite the calibration, the overall model performance for the N load was better than for the P load (Figure 49, Table 13). Stations with only monthly sampling were especially prone to large deviations. Due to the high uncertainty in observed P loads, we excluded 16 stations at the upper Danube and the Alpine tributaries with less than 22 samples per year.¹¹

¹¹ The threshold is similar to the validation for the previous DRBMP.

Model deviations can have various causes and individual cases need specific assessments to identify and overcome these issues. Some aspects are presented below.

- Model and data limitations of large-scale applications

The mobilization and relocation of nutrients in river basins is complex because many factors are involved and many processes interact at different scales. Any model simplifies reality, in particular if it has to be applied to large, international, and heterogeneous river basins such as the DRB. Large model deviations likely occur in catchments (or in years) which deviate from the (average) conditions represented by the model. This is especially true for the hydrology of tributaries where the relative errors of the HYPE model were largest, also after our adjustment. However, it remains unclear to which degree the emissions and the in-stream retention contribute to model deviations as an independent validation is impossible at the basin-scale.

The decision to use national datasets (if at all available) for the modelling of nutrient emissions was a trade-off between the resources needed for the data collection and preprocessing, the acceptance of results, and the consistency among countries. Some important model input is hardly available or only as mean values, e.g. the efficacy of waste-water treatment in DCTP or the soil erosion in Alpine catchments. For regionally important processes like gully erosion, quantitative data is simply unavailable. Additionally, the hydrology in the DRB is complex with hydro-power plants, reservoirs, canals. To consider the human impact adequately, more information on the management would be needed as it may strongly influence the in-stream mobilization and retention of nutrients. Last not least, the nutrient remobilization and concentrations in river systems may also depend on their availability. They can sharply decline after floods empty internal stocks, and these stocks can require many years to restore (Zoboli et al., 2015).

Some of the stations excluded due to low sampling frequencies also had small catchments (e.g. at r. Paar in DE-BY). Even with more reliable observed loads, the model deviations are likely to remain most problematic here due to the available data (resolution) leading to high relative errors even if the absolute errors are small. Therefore, the model validation is limited to sufficiently large station catchments (i.e. tributaries).

- Temporal resolution of model (data)

The monthly and annual input data and the model time steps as well as the rare samplings may not capture extreme rainfall and floods. Such events occur over short periods (sub-daily to a few days) and may transport considerable amounts of the annual load, and can even change multi-annual mean values. For instance, the average annual P load in r. Someş (TNMN station RO12) was strongly underestimated by MONERIS. The peak concentrations of 1.9 mg P/l in January 2016 and 1.3 mg P/l in February 2016 resulted in a bi-monthly P load of about 1500 t which is more than 80% of the combined load of the years 2015, 2017, and 2018. These two events increased the average load from 592 t/yr to 937 t/yr and hence the model deviation (312 t/yr).

- Uncertainty and inconsistencies in observation data

Many sources of uncertainty in observation data exist of which the representativeness in space and time (where, when, how often sampled) is of high importance (Rode and Suhr, 2007). This is supported deviating annual loads over short distances where the sampling frequency is low (Figure 50). This uncertainty might be further enhanced by different national regulations. For instance, the Bulgarian concentrations at TNMN stations along the Danube were higher than the Romanian values (not shown). Despite high sampling frequencies, the P loads at Hainburg (TNMN code AT6) and Bratislava

(TNMN code SK1) changed from 2.5 kt (AT6) to 6.7 kt further downstream at SK1. Although both stations are located in the same AU, only the time-series for AT6 was complete. Given the unknown uncertainty, we generally consider model deviations of 30% as acceptable.

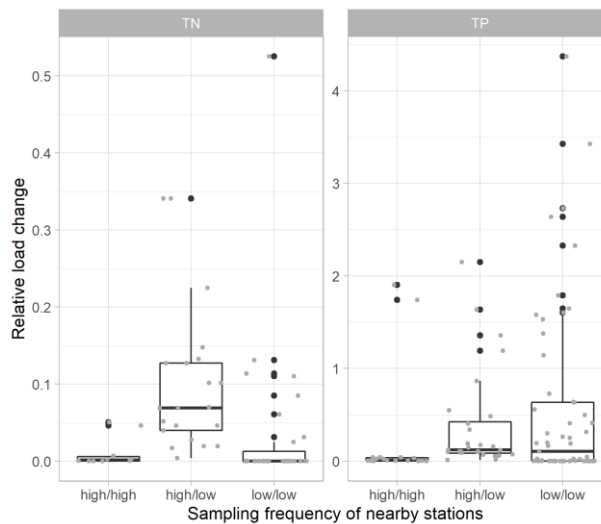


Figure 50. The uncertainty in 163 paired annual loads (left: TN, right: TP) – expressed as relative change in calculated loads for neighboring stations – depends on the sampling frequency (high ≥ 20 samples/yr, low < 20 samples/yr). Zero means perfect agreement, one that one load is twice the other one.

3.4 Scenario results

Significant changes in emissions and loads to the reference situation were observed for the Vision scenarios, except for wet-year Vision III (Figure 51). While the annual emissions decreased by 33 kt N (6.4%) and 2.4 kt P (7.7%) in the Baseline scenario, the measures for Vision I resulted in reductions of 115 kt N (22%) and 7.4 kt P (24%, Figures 52-53). More efficient riparian buffers (Vision II) could retain another 9 kt N and 1.7 kt P which corresponded to 24% and 30% lower nutrient emission compared to the reference period.

Hydrology had a stronger impact on emissions than the efficiency of riparian buffers which were limited to emissions via soil erosion and surface runoff. The dry-year scenario decreased the Vision emission by 37 kt N (-30% to reference period) and 2.4 kt P (-32%). Under the high-flow conditions in the wet-year scenario – the DRB suffered severe flood events in many tributaries throughout the selected year 2010 (International Commission for the Protection of the Danube River, 2012) – the emissions sharply increased and almost equaled the effect of the visionary measures. The emission increased by 95 kt N and 5.3 kt P compared to the Vision scenario which means 20 kt N (4%) and 2.2 kt P (7%) lower emission than in the reference period.

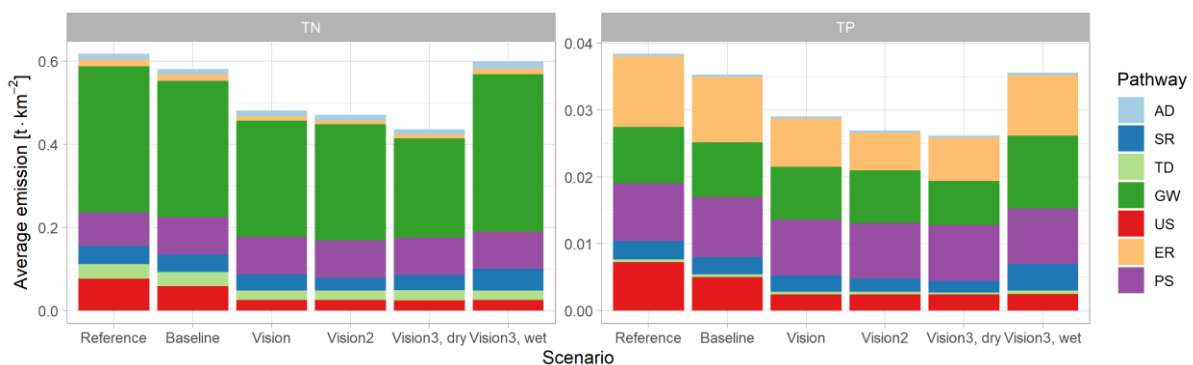


Figure 51. Area-specific basin-wide nutrient emission for the reference period and the scenarios.

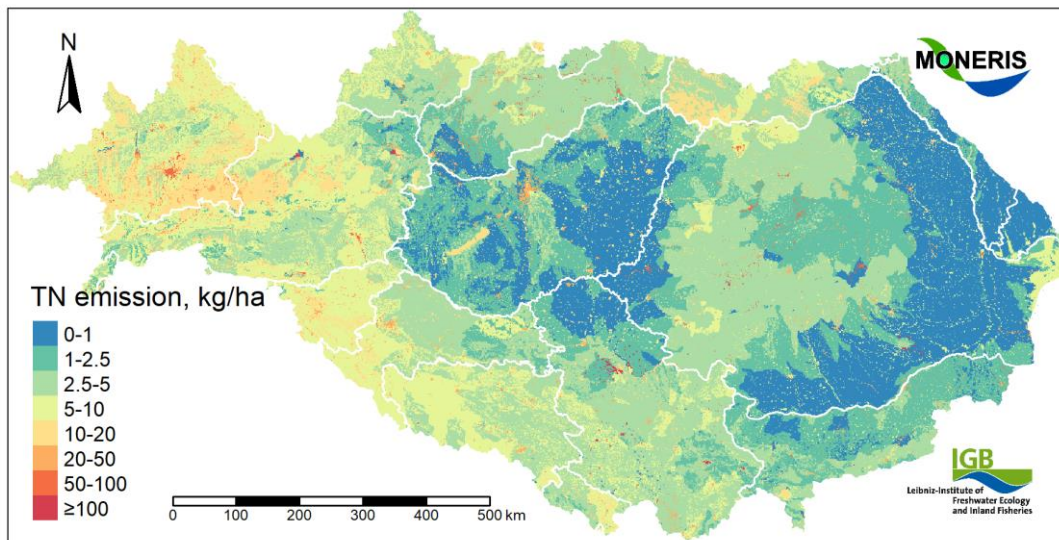


Figure 52. Mean N emission disaggregated by land use for the Vision scenario (cf. Figure 27 for the reference period). Artefacts may arise due to inconsistent input data (e.g. gridded population and urban areas) as well as point sources assigned to discharge points.

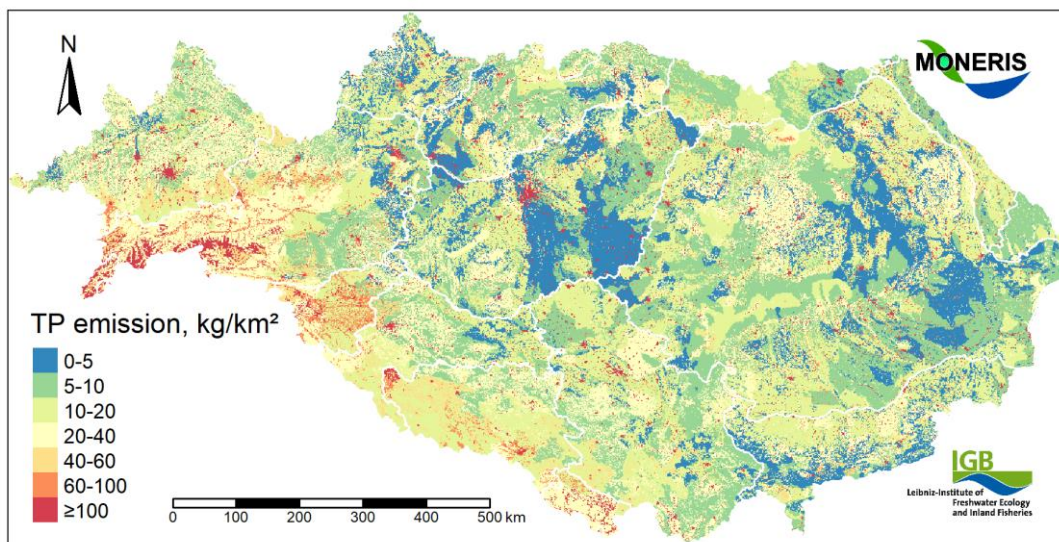


Figure 53. Mean P emission disaggregated by land use for the Vision scenario (cf. Figure 28 for the reference period). Artefacts may arise due to inconsistent input data (e.g. gridded population and urban areas) as well as point sources assigned to discharge points.

Considering the limitations of monthly data and calculations to represent the erosivity of rainfall peaks as well as the transport capacity during flow peaks, it is very likely that the model underestimated the emissions and the resulting loads for the wet-year scenario. In the light of floods with recurrence intervals of up to 100 years (and locally even beyond), high nutrient emissions may seem less important compared to damages and casualties. Nonetheless, the wet- and dry-scenarios exemplify how the emissions may change under moderate to strong climate changes.

As expected, the change pattern was similar for emissions and loads (Figure 54). Under the tested wet-year conditions, the in-stream retention was lower than during the reference period, especially for P. Despite lower emissions, the loads were higher. The impacts on the emissions varied considerably among the pathways. The measures strongly lowered the emissions via urban systems and soil erosion (Figure 55). As these pathways were of different relevance for N and P as well as for the countries, the scenario effects also varied among the countries. In addition, the observed variability (Table C in the

Appendix) was also the result of the different reference conditions including the hydrological situation in the dry- and wet years for the Vision III scenarios. Without taking hydrological (and e.g. demographic changes) into consideration, the target concentrations and loads for the Black Sea would be reachable with the tested measures.

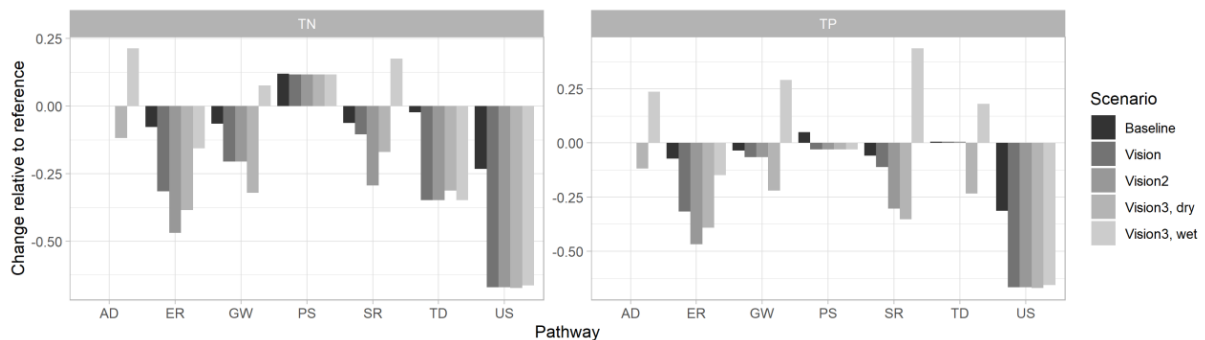


Figure 54. Relative load change at Reni to the reference period with absolute loads in kt.

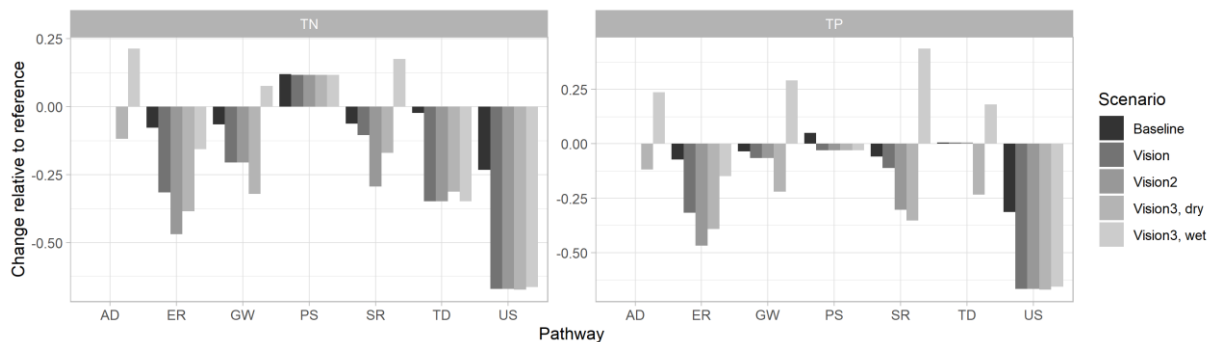


Figure 55. Change of pathways for the scenarios relative to the reference period.

3.5 Conclusions and recommendations

- The comprehensive data revision makes the estimation of nutrient fluxes in the DRB more reliable and improves the understanding of nutrient pathways and sources.
- Agricultural land (arable and grassland) and urban areas contribute more than 30% of the N and P emissions which makes them the dominant nutrient sources. Groundwater and soil erosion are the main pathways for N and P, respectively, followed for both by urban systems and point sources.
- This dominance is in agreement with earlier MONERIS applications. However, the noticeable data change hampers quantitative comparisons of emissions and loads to previous results.
- The loads and concentrations exported to the Black Sea are already close to the target values. They can significantly be reduced by consequently reducing the agricultural N surplus, expanding the conservation of agricultural soils, and improving the waste-water collection and treatment. However, these measures may become less effective if intense rainfall and high-flood events become more frequent. Additional measures like more buffer strips in NVZ are also important as they provide other positive effects (e.g. shading, habitats).
- It is important to note that the model validation is limited to load comparisons. The reliability of observed loads depends on the sampling frequency. TN and TP are typically only sampled monthly. More bi-weekly sampling along the (main) tributaries is recommended to improve the model validation and better identify model limitations in the future.

- This would be especially helpful for TP. More observation data, including suspended solids, is required to increase the reliability of the re-calibrated retention approach in future studies.
- The collection of country data via ICPDR is extremely useful but still time consuming. It would be helpful to start in advance to have (more) time to fill gaps and to discuss assumptions e.g. on the independent waste-water collection and treatment systems.
- Various problems may arise when setting up the model. The regular exchange with PM EG and NTG as well as the ad-hoc MONERIS WG is helpful and should be continued.
- We recommend conducting more plausibility checks of officially reported data – by national authorities as well as ICPDR (e.g. coordinates of agglomerations in the UWWTD inventory, industrial discharges, consistency of boundaries, measured data in TNMN). This would also be beneficial for other purposes.
- The model is based on international and national data. Although the latter fosters the acceptance of model results, such data is not available everywhere or may differ in resolution, type, and underlying assumptions. This limits the comparison of country results.
- Future steps towards a more harmonized database could aim at the calculation of regional N balances and the modelling of hydrology – two key input datasets. The centralized calculations of N balances at BOKU Vienna could be extended to all countries. The availability of modelled water fluxes for the reference period is a prerequisite for overcoming general limitations of estimating the runoff at AU level from (observed or modelled) water discharge. This may require a better integration of these model results into MONERIS. Both also allow more refined scenarios (e.g. on fertilizer application or climate change).
- The model resolution of MONERIS and the hydrological model should be (more) consistent, at least with common boundaries of the DRB. We recommend to further increase the number of AUs as large AUs may blur the spatial pattern of nutrient emissions. Ideally, well-established monitoring stations are located close to the outlet of AUs. The AU areas in different countries could be harmonized.

3.6 Acknowledgements

The work was partly funded by the Danube Transnational Programme (Project “Improving water quality in the Danube river and its tributaries by integrative floodplain management based on Ecosystem Services”, DTP3-389-2.1 – IDES, <https://www.interreg-danube.eu/approved-projects/ides>).

We are especially thankful to Ottavia Zoboli (BOKU Vienna) for providing the regional N balances for various countries, to Elisabeth Bondar-Kunze (BOKU Vienna) who made the free access to the Austrian precipitation data possible, and to Jos van Gils (Deltares) who shared the HYPE results for the Danube basin. Last but not least, we are grateful to ICPDR (Adam Kovacs, Zoran Major, Alex Höbart) and all members of PM EG and NTG who supported the modelling in many ways.

The modelling would be impossible without many national and international data providers and statistical offices. We happily acknowledge the E-OBS dataset from the EU-FP6 project UERRA (<https://www.uerra.eu>) and the Copernicus Climate Change Service, and the data providers in the ECA&D project (<https://www.ecad.eu>), the soil-loss maps from the European Soil Data Centre (ESDAC), European Commission, Joint Research Centre (<https://esdac.jrc.ec.europa.eu>), as well as the EMEP data from the Norwegian Meteorological Institute. Eurostat thankfully provided revised net balances for Slovakia.

4 References

- Borrelli, P., Alewell, C., Alvarez, P., Anache, J. A. A., Baartman, J., Ballabio, C., Bezak, N., Biddoccu, M., Cerdà, A., Chalise, D., Chen, S., Chen, W., De Girolamo, A. M., Gessesse, G. D., Deumlich, D., Diodato, N., Efthimiou, N., Erpul, G., Fiener, P., Freppaz, M., Gentile, F., Gericke, A., Haregeweyn, N., Hu, B., Jeanneau, A., Kaffas, K., Kiani-Harchegani, M., Villuendas, I. L., Li, C., Lombardo, L., López-Vicente, M., Lucas-Borja, M. E., Märker, M., Matthews, F., Miao, C., Mikoš, M., Modugno, S., Möller, M., Naipal, V., Nearing, M., Owusu, S., Panday, D., Patault, E., Patriche, C. V., Poggio, L., Portes, R., Quijano, L., Rahdari, M. R., Renima, M., Ricci, G. F., Rodrigo-Comino, J., Saia, S., Samani, A. N., Schillaci, C., Syrris, V., Kim, H. S., Spinola, D. N., Oliveira, P. T., Teng, H., Thapa, R., Vantas, K., Vieira, D., Yang, J. E., Yin, S., Zema, D. A., Zhao, G. & Panagos, P. 2021. Soil erosion modelling: A global review and statistical analysis. *Science of The Total Environment*, 780, 146494, doi: 10.1016/j.scitotenv.2021.146494.
- Borrelli, P., Robinson, D. A., Fleischer, L. R., Lugato, E., Ballabio, C., Alewell, C., Meusburger, K., Modugno, S., Schütt, B., Ferro, V., Bagarello, V., Oost, K. V., Montanarella, L. & Panagos, P. 2017. An assessment of the global impact of 21st century land use change on soil erosion. *Nature Communications*, 8, 2013, doi: 10.1038/s41467-017-02142-7.
- Carl, P. & Behrendt, H. 2008. Regularity-based functional streamflow disaggregation: 1. Comprehensive foundation. *Water Resources Research*, 44, W02420, doi: 10.1029/2004WR003724.
- Carl, P., Gerlinger, K., Hattermann, F. F., Krysanova, V., Schilling, C. & Behrendt, H. 2008. Regularity-based functional streamflow disaggregation: 2. Extended demonstration. *Water Resources Research*, 44, W03426, doi: 10.1029/2006WR005056.
- Cornes, R. C., van der Schrier, G., van den Besselaar, E. J. M. & Jones, P. D. 2018. An Ensemble Version of the E-OBS Temperature and Precipitation Data Sets. *Journal of Geophysical Research: Atmospheres*, 123, 9391-9409, doi: 10.1029/2017JD028200.
- ECA&D 2021. *E-OBS ensemble mean version 22.0e (0.1 deg. regular grid)* [Online]. Copernicus Climate Change Service (C3S). Available: https://surfobs.climate.copernicus.eu/dataaccess/access_eobs.php.
- European Environment Agency 2012. *EEA Catchments and Rivers Network System ECRINS v1.1 - Rationales, building and improving for widening uses to Water Accounts and WISE applications*, EEA Technical report 7/2012, Copenhagen, 111 pp. doi: 10.2800/51667 Available: https://www.eea.europa.eu/ds_resolveuid/P2Z9F5AHUV.
- European Environment Agency 2020. *The European Pollutant Release and Transfer Register (E-PRTR), Member States reporting under Article 7 of Regulation (EC) No 166/2006*. Available: <https://www.eea.europa.eu/data-and-maps/data/member-states-reporting-art-7-under-the-european-pollutant-release-and-transfer-register-e-prtr-regulation-23>.
- European Environment Agency 2021a. *Corine Land Cover (CLC) 2018, Version 2020_20u1*. Available: <https://land.copernicus.eu/pan-european/corine-land-cover/clc2018>.
- European Environment Agency 2021b. *Industrial Reporting under the Industrial Emissions Directive 2010/75/EU and European Pollutant Release and Transfer Register Regulation (EC) No 166/2006*. Available: <https://www.eea.europa.eu/data-and-maps/data/industrial-reporting-under-the-industrial-2>.
- Eurostat 2021a. *Gross nutrient balance [aei_pr_gnb]* [Online]. Available: https://appsso.eurostat.ec.europa.eu/nui/show.do?lang=en&dataset=aei_pr_gnb [Accessed 23.6.2021].
- Eurostat 2021b. *Population connected to wastewater treatment plants [env_ww_con]* [Online]. Available: https://appsso.eurostat.ec.europa.eu/nui/show.do?lang=en&dataset=env_ww_con [Accessed 10.3.2021].
- Federal Environment Agency 2021. *thru.de* [Online]. Available: <https://www.thru.de/thrude/>.
- Federal Institute for Geosciences and Natural Resources 2019. *Hydrogeology of Germany 1:1,000,000 (HY1000)*, 1. Available:

- https://www.bgr.bund.de/DE/Themen/Wasser/Projekte/abgeschlossen/Beratung/Had/had_projektbeschr.html?nn=1542268.
- Federal Institute for Geosciences and Natural Resources & German State Geological Surveys 2019. *Hydrogeological Map of Germany 1:250,000 (HÜK250)*, 1.0.3. Available: https://www.bgr.bund.de/DE/Themen/Wasser/Projekte/laufend/Beratung/Huek200/huek200_projektbeschr.html.
- Federal Institute for Geosciences and Natural Resources & United Nations Educational, Scientific and Cultural Organization 2019. *IHME1500 - International Hydrogeological Map of Europe 1:1,500,000*, 1.2. Available: https://www.bgr.bund.de/EN/Themen/Wasser/Projekte/laufend/Beratung/Ihme1500/ihme1500_projektbeschr_en.html.
- Federal Ministry of Agriculture, Regions and Tourism 2020. *Fließgewässer des Gesamtwässernetz Österreich (GGN)* [Online]. Environment Agency Austria. Available: <https://www.data.gv.at/katalog/dataset?tags=Gew%C3%A4ssernetz>.
- Federal Office of the Environment 2021. *SwissPRTR pollutant register* [Online]. Available: <https://www.bafu.admin.ch/bafu/en/home/topics/chemicals/state/swissprtr-pollutant-register.html>.
- Fischer, P., Pöthig, R. & Venohr, M. 2017. The degree of phosphorus saturation of agricultural soils in Germany: Current and future risk of diffuse P loss and implications for soil P management in Europe. *Science of The Total Environment*, 599-600, 1130-1139, doi: 10.1016/j.scitotenv.2017.03.143.
- GeoBasis-DE & Federal Agency for Cartography and Geodesy 2013. *Digitales Landschaftsmodell 1 : 250.000 - DLM250 (AAA)*, 2013. Available: <https://gdz.bkg.bund.de/index.php/default/digitale-geodaten/digitale-landschaftsmodelle/digitales-basis-landschaftsmodell-ebenen-basis-dlm-ebenen.html>.
- geofabrik GmbH & OpenStreetMap Contributors 2018. Available: <https://download.geofabrik.de/europe.html>.
- Gericke, A., Nguyen, H. H., Fischer, P., Kail, J. & Venohr, M. 2020. Deriving a Bayesian Network to Assess the Retention Efficacy of Riparian Buffer Zones. *Water*, 12, 617, doi: 10.3390/w12030617.
- Heidecke, C., Hirt, U., Kreins, P., Kuhr, P., Kunkel, R., Mahnkopf, J., Schott, M., Tetzlaff, B., Venohr, M., Wagner, A. & Wendland, F. 2015. *Entwicklung eines Instrumentes für ein flussgebietsweites Nährstoffmanagement in der Flussgebietseinheit Weser*, Final report, Thünen Report 21, Braunschweig, Johann Heinrich von Thünen-Institut, 380 p.
- Hirt, U., Wetzig, A., Devandra Amatya, M. & Matranga, M. 2011. Impact of Seasonality on Artificial Drainage Discharge under Temperate Climate Conditions. *International Review of Hydrobiology*, 96, 561-577, doi: 10.1002/iroh.201111274.
- International Commission for the Protection of the Danube River 2012. *2010 Floods in the Danube River Basin - Brief overview of key events and lessons learned*, Vienna, ICPDR, 18 pp. Available: https://www.icpdr.org/main/sites/default/files/nodes/documents/icpdr_flood_report_2010.pdf.
- Ionita, I., Niacsu, L., Poesen, J. & Fullen, M. A. 2021. Controls on the development of continuous gullies: A 60 year monitoring study in the Moldavian Plateau of Romania. *Earth Surface Processes and Landforms*, 46, 2746-2763, doi: 10.1002/esp.5204.
- Kertész, Á. & Gergely, J. 2011. Gully erosion in Hungary, review and case study. *Procedia Social and Behavioral Sciences*, 19, 693-701, doi: 10.1016/j.sbspro.2011.05.187.
- Länderinitiative Kernindikatoren 2020. *Stickstoffüberschüsse der landwirtschaftlich genutzten Fläche in Deutschland (Flächenbilanz)* [Online]. LIKI. Available: <https://www.lanuv.nrw.de/liki/index.php?mode=indi&indikator=10>.
- Lemm, J. U., Venohr, M., Globevnik, L., Stefanidis, K., Panagopoulos, Y., van Gils, J., Posthuma, L., Kristensen, P., Feld, C. K., Mahnkopf, J., Hering, D. & Birk, S. 2021. Multiple stressors determine river ecological status at the European scale: Towards an integrated understanding of river status deterioration. *Global Change Biology*, 27, 1962-1975, doi: 10.1111/gcb.15504.

- Ministry of Agriculture, F. a. F. 2019. *Unified state register of irrigation and drainage systems (KatMeSiNa)* [Online]. Available: <https://podatki.gov.si/dataset/evidenca-melioracijskih-sistemov-in-naprav-katmesina/resource/9ef8cb3a-b9a0-4466-8ab4-68e50f0301ed>.
- Norwegian Meteorological Institute 2019. *EMEP MSC-W modelled air concentrations and depositions*, program version 4.33. Available: https://emep.int/mscw/mscw_moddata.html.
- Norwegian Meteorological Institute 2020. *EMEP MSC-W modelled air concentrations and depositions*, program version 4.35. Available: https://emep.int/mscw/mscw_moddata.html.
- OECD 2021. *Agri-Environmental indicators: Nutrients: Nitrogen balance* [Online]. Available: <https://stats.oecd.org/#>.
- Panagos, P., Borrelli, P., Poesen, J., Ballabio, C., Lugato, E., Meusburger, K., Montanarella, L. & Alewell, C. 2015. The new assessment of soil loss by water erosion in Europe. *Environmental Science & Policy*, 54, 438-447, doi: 10.1016/j.envsci.2015.08.012.
- Rode, M. & Suhr, U. 2007. Uncertainties in selected river water quality data. *Hydrology and Earth System Sciences*, 11, 863-874, doi: 10.5194/hess-11-863-2007.
- Schiavina, M., Freire, S. & MacManus, K. 2019. *GHS population grid multitemporal (1975-1990-2000-2015)*, R2019A. Available: <http://data.europa.eu/89h/0c6b9751-a71f-4062-830b-43c9f432370f>.
- Schick, J., Kratz, S., Rückamp, D., Shwiekh, R., Haneklaus, S. & Schnug, E. 2013. *Comparison and Inter-Calibration of Different Soil P Tests Used in the Baltic Sea Countries*, Baltic Manure Knowledge Report, Braunschweig, Germany, 47 pp.
- Swedish Meteorological and Hydrological Institute 2020. *The HYPE wiki pages* [Online]. Norrköping, SE: SMHI. Available: <http://www.smhi.net/hype/wiki/doku.php>.
- Vadas, P. A., Kleinman, P. J. A., Sharpley, A. N. & Turner, B. L. 2005. Relating Soil Phosphorus to Dissolved Phosphorus in Runoff: A Single Extraction Coefficient for Water Quality Modeling. *Journal of Environmental Quality*, 34, 572-580, doi: 10.2134/jeq2005.0572.
- van Gils, J., Posthuma, L., Cousins, I. T., Brack, W., Altenburger, R., Baveco, H., Focks, A., Greskowiak, J., Kühne, R., Kutsarova, S., Lindim, C., Markus, A., van de Meent, D., Munthe, J., Schueder, R., Schüürmann, G., Slobodnik, J., de Zwart, D. & van Wezel, A. 2020. Computational material flow analysis for thousands of chemicals of emerging concern in European waters. *Journal of Hazardous Materials*, 397, 122655, doi: 10.1016/j.jhazmat.2020.122655.
- Vanmaercke, M., Panagos, P., Vanwalleghem, T., Hayas, A., Foerster, S., Borrelli, P., Rossi, M., Torri, D., Casali, J., Borselli, L., Vigiak, O., Maerker, M., Haregeweynm, N., Geeter, S. D., Zgłobicki, W., Bielders, C., Cerdà, A., Conoscenti, C., Figueiredo, T. d., Evans, B., Golosov, V., Ionita, I., Karydas, C., Kertész, A., Krása, J., Bouteiller, C. L., Radoane, M., Ristić, R., Rouseva, S., Stankoviansky, M., Stolte, J., Stolz, C., Bartley, R., Wilkinson, S., Jarihani, B. & Poesen, J. 2021. Measuring, modelling and managing gully erosion at large scales - A state of the art. *Earth-Science Reviews*, 218, 103637, doi: 10.1016/j.earscirev.2021.103637.
- Venohr, M., Hirt, U., Hofmann, J., Opitz, D., Gericke, A., Wetzig, A., Natho, S., Neumann, F., Hürdler, J., Matranga, M., Mahnkopf, J., Gadegast, M. & Behrendt, H. 2011. Modelling of Nutrient Emissions in River Systems – MONERIS – Methods and Background. *International Review of Hydrobiology*, 96, 435-483, doi: 10.1002/iroh.201111331.
- Verheijen, F. G. A., Jones, R. J. A., Rickson, R. J. & Smith, C. J. 2009. Tolerable versus actual soil erosion rates in Europe. *Earth-Science Reviews*, 94, 23-38, doi: 10.1016/j.earscirev.2009.02.003.
- Wilke, B. & Schaub, D. 1996. Phosphatanreicherung bei Bodenerosion. In: Hugenroth, P. (ed.) *Mitteilungen der Deutschen Bodenkundlichen Gesellschaft*, Vol. 79. Oldenburg: Deutsche Bodenkundliche Gesellschaft, 435-438.
- Zoboli, O., Viglione, A., Rechberger, H. & Zessner, M. 2015. Impact of reduced anthropogenic emissions and century flood on the phosphorus stock, concentrations and loads in the Upper Danube. *Science of The Total Environment*, 518-519, 117-129, doi: 10.1016/j.scitotenv.2015.02.087.

5 Appendix

Table A. Pathways of TN emissions for ICPDR countries (catchment area > 2000 km²), 2015–2018. AD = atmospheric deposition on surface waters, SR = surface runoff, ER = soil erosion, TD = tile drainages, GW = groundwater, US = urban systems, PS = waste-water treatment plants and industrial dischargers. Abs = absolute values in 1000 km² (area) and t/yr (emission), pc = share of country on total DRB (area or emission), and sp = area-specific emission in kg/ha/yr.

Country	Area		AD			SR			ER			TD			GW			US			PS			Total		
	abs	pc	abs	pc	sp	abs	pc	sp	abs	pc	sp	abs	pc	sp	abs	pc	sp	abs	pc	sp	abs	pc	sp	abs	pc	sp
AT	80.6	10	1956	16.4	0.2	5939	16.2	0.7	3966	29.5	0.5	2283	7.9	0.3	39551	13.6	4.9	1194	1.9	0.1	9594	14.6	1.2	64489	12.6	8
BA	38.2	4.7	369	3.1	0.1	2851	7.8	0.7	419	3.1	0.1	200	0.7	0.1	26087	9	6.8	9037	14.1	2.4	907	1.4	0.2	39881	7.8	10.4
BG	47.2	5.8	167	1.4	0	662	1.8	0.1	1026	7.6	0.2	1532	5.3	0.3	13660	4.7	2.9	3849	6	0.8	2759	4.2	0.6	23693	4.6	5
CZ	21.7	2.7	176	1.5	0.1	1019	2.8	0.5	240	1.8	0.1	4179	14.5	1.9	12571	4.3	5.8	1704	2.7	0.8	1645	2.5	0.8	21549	4.2	9.9
DE	56.3	7	1666	14	0.3	5203	14.2	0.9	301	2.2	0.1	13504	46.9	2.4	39764	13.7	7.1	1157	1.8	0.2	11101	16.8	2	72544	14.1	12.9
HR	35	4.3	572	4.8	0.2	2322	6.3	0.7	242	1.8	0.1	2739	9.5	0.8	18376	6.3	5.2	3574	5.6	1	2833	4.3	0.8	30731	6	8.8
HU	93	11.5	1480	12.4	0.2	1787	4.9	0.2	633	4.7	0.1	365	1.3	0	8255	2.8	0.9	1495	2.3	0.2	8230	12.5	0.9	22801	4.4	2.5
MD	12.4	1.5	33	0.3	0	96	0.3	0.1	150	1.1	0.1	113	0.4	0.1	1184	0.4	1	1677	2.6	1.3	373	0.6	0.3	3671	0.7	3
ME	6.9	0.9	141	1.2	0.2	786	2.1	1.1	27	0.2	0	16	0.1	0	4219	1.5	6.1	337	0.5	0.5	123	0.2	0.2	5648	1.1	8.1
RO	238.4	29.5	3095	26	0.1	6664	18.2	0.3	3787	28.2	0.2	1070	3.7	0	52575	18.1	2.2	12577	19.6	0.5	14607	22.2	0.6	95134	18.5	4
RS	82	10.1	746	6.3	0.1	3474	9.5	0.4	556	4.1	0.1	647	2.2	0.1	35631	12.2	4.3	17603	27.4	2.1	6908	10.5	0.8	65649	12.8	8
SI	16.4	2	441	3.7	0.3	1683	4.6	1	484	3.6	0.3	251	0.9	0.2	10480	3.6	6.4	1977	3.1	1.2	1349	2	0.8	16620	3.2	10.1
SK	47.1	5.8	442	3.7	0.1	2113	5.8	0.4	516	3.8	0.1	1286	4.5	0.3	15706	5.4	3.3	3764	5.9	0.8	4051	6.1	0.9	27650	5.4	5.9
UA	30.6	3.8	579	4.9	0.2	1933	5.3	0.6	96	0.7	0	506	1.8	0.2	11446	3.9	3.7	4339	6.7	1.4	1185	1.8	0.4	20121	3.9	6.6

Table B. Pathways of TP emissions for ICPDR countries (catchment area > 2000 km²), 2015–2018. AD = atmospheric deposition on surface waters, SR = surface runoff, ER = soil erosion, TD = tile drainages, GW = groundwater, US = urban systems, PS = waste-water treatment plants and industrial dischargers. Abs = absolute values in 1000 km² (area) and t/yr (emission), pc = share of country on total DRB (area or emission), and sp = area-specific emission in kg/ha/yr.

Country	Area		AD			SR			ER			TD			GW			US			PS			Total		
	abs	pc	abs	pc	sp	abs	pc	sp	abs	pc	sp	abs	pc	sp	abs	pc	sp	abs	pc	sp	abs	pc	sp	abs	pc	sp
AT	80.6	10	44	15.1	0	447	20	0.1	2389	27.9	0.3	17	5.1	0	997	14.6	0.1	215	3.6	0	643	9.2	0.1	4748	15.3	0.6
BA	38.2	4.7	12	4.1	0	254	11.4	0.1	297	3.5	0.1	4	1.3	0	552	8.1	0.1	839	14.2	0.2	200	2.9	0.1	2157	6.9	0.6
BG	47.2	5.8	5	1.9	0	28	1.3	0	848	9.9	0.2	10	3.1	0	167	2.4	0	298	5.1	0.1	357	5.1	0.1	1714	5.5	0.4
CZ	21.7	2.7	3	1.2	0	39	1.7	0	159	1.9	0.1	16	5	0	137	2	0.1	135	2.3	0.1	129	1.8	0.1	618	2	0.3
DE	56.3	7	21	7.2	0	238	10.7	0	275	3.2	0	133	40.6	0	567	8.3	0.1	173	2.9	0	731	10.5	0.1	2128	6.8	0.4
HR	35	4.3	13	4.6	0	153	6.8	0	194	2.3	0.1	29	8.9	0	356	5.2	0.1	494	8.4	0.1	740	10.6	0.2	1978	6.4	0.6
HU	93	11.5	36	12.3	0	70	3.1	0	463	5.4	0	5	1.6	0	531	7.8	0.1	260	4.4	0	1277	18.3	0.1	2641	8.5	0.3
MD	12.4	1.5	1	0.3	0	4	0.2	0	114	1.3	0.1	4	1.4	0	58	0.8	0	125	2.1	0.1	113	1.6	0.1	419	1.3	0.3
ME	6.9	0.9	8	2.6	0	121	5.4	0.2	15	0.2	0	1	0.2	0	174	2.5	0.3	26	0.4	0	26	0.4	0	370	1.2	0.5
RO	238.4	29.5	90	30.7	0	317	14.2	0	2074	24.2	0.1	25	7.7	0	1434	21	0.1	1104	18.7	0	1525	21.9	0.1	6567	21.1	0.3
RS	82	10.1	21	7.2	0	229	10.3	0	397	4.6	0	9	2.7	0	892	13	0.1	1500	25.4	0.2	547	7.8	0.1	3595	11.6	0.4
SI	16.4	2	9	3	0	131	5.9	0.1	325	3.8	0.2	8	2.3	0	268	3.9	0.2	214	3.6	0.1	213	3.1	0.1	1161	3.7	0.7
SK	47.1	5.8	10	3.5	0	99	4.4	0	368	4.3	0.1	55	16.9	0	363	5.3	0.1	234	4	0	296	4.2	0.1	1411	4.5	0.3
UA	30.6	3.8	16	5.5	0	76	3.4	0	53	0.6	0	10	3	0	281	4.1	0.1	271	4.6	0.1	139	2.0	0	847	2.7	0.3

Table C. Country-specific changes in % of nutrient emission for the scenarios and reference emission in tons. The values for the Vision III scenarios reflect the different hydrological conditions in the selected wet- and dry-years compared to the average conditions.

Country	TN						TP					
	Baseline	Vision1	Vision2	Vision3, dry	Vision3, wet	Reference	Baseline	Vision1	Vision2	Vision3, dry	Vision3, wet	Reference
AT	2.9	-5.4	-8.7	-13.7	-2.5	64489	-5.8	-9.3	-22	-15.3	-4.9	4748
BA	-8.7	-41	-42.6	-50.4	-24.2	39881	-7.9	-47.5	-52	-61.1	-19	2157
BG	-15.6	-34.6	-35.1	-38.7	-16.9	23693	-14.7	-33.3	-36.7	-38.9	-24	1714
CZ	-5.2	-42.1	-42.6	-44.7	-33.1	21549	-17.2	-26.7	-29	-29.7	2.2	618
DE	4	-19.8	-21.5	-22.4	-12.9	72544	-2.3	-6.6	-11.4	-11.7	2.4	2128
HR	-18.4	-32.5	-32.7	-50.2	3.9	30731	-47.1	-50.4	-50.6	-58.7	-26	1978
HU	-1.9	2.8	1.3	-9.1	86.5	22801	-10.4	-16	-18.1	-22.7	6.8	2641
MD	-15.1	-30.2	-31.5	-29.1	-12.8	3671	-23.9	-43.7	-48	-47	-27	419
ME	-3.4	-24.7	-27.6	-28.2	-11.4	5648	-0.8	-13.9	-21.2	-30.3	22.4	370
RO	-16.8	-20	-22.1	-25.9	-2	95134	-5.4	-14.6	-20.6	-23.2	2.7	6567
RS	-0.4	-36.4	-37.6	-43.3	-18.5	65649	14.9	-39.7	-42.6	-46.5	-28.3	3595
SI	-20	-13.4	-16	-24.4	0.1	16620	-30.1	-39.3	-45.7	-51.9	-21.3	1161
SK	-8.6	-9.8	-10.6	-16.7	17.7	28861	-3	-13.8	-16.4	-22.5	33	1474
UA	-2.6	-16.2	-18.1	-26.4	6.2	20121	-13.4	-48.9	-51.9	-55.5	-27.9	847